

# Synthesis of titanium borylimido compounds supported by diamide-amine ligands and their reactions with alkynes

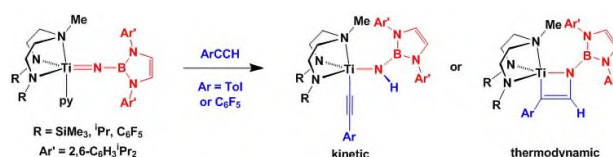
Benjamin A. Clough and Philip Mountford\*

Chemistry Research Laboratory, Department of Chemistry, University of Oxford, Mansfield Road, Oxford OX1 3TA, UK. E-mail: philip.mountford@chem.ox.ac.uk

## Abstract

We report a combined synthetic, mechanistic and computational (DFT) study of the synthesis of new diamide-amine supported titanium borylimides and their reactions with TolCCH and Ar<sup>F</sup>CCH (Tol = 4-C<sub>6</sub>H<sub>4</sub>Me, Ar<sup>F</sup> = C<sub>6</sub>F<sub>5</sub>). Reaction of Ti{NB(NAr'CH)<sub>2</sub>}Cl<sub>2</sub>(py)<sub>3</sub> (Ar' = 2,6-C<sub>6</sub>H<sub>3</sub><sup>i</sup>Pr<sub>2</sub>) with Li<sub>2</sub>N<sub>2</sub><sup>R</sup>N<sup>Me</sup> (N<sub>2</sub><sup>R</sup>N<sup>Me</sup> = MeN(CH<sub>2</sub>CH<sub>2</sub>NR)<sub>2</sub>) or Li<sub>2</sub>N<sub>2</sub>N<sup>py</sup> (N<sub>2</sub>N<sup>py</sup> = (2-C<sub>5</sub>H<sub>4</sub>N)CMe(CH<sub>2</sub>NSiMe<sub>3</sub>)<sub>2</sub>) afforded the borylimides Ti(N<sub>2</sub><sup>R</sup>N<sup>Me</sup>){NB(NAr'CH)<sub>2</sub>}(py) (R = SiMe<sub>3</sub> (**9**) Ar<sup>F</sup> (**10**) or <sup>i</sup>Pr (**11**)) and Ti(N<sub>2</sub>N<sup>py</sup>){NB(NAr'CH)<sub>2</sub>}(py) (**21**). Compounds **9** and **10** reacted with ArCCH (Ar = Ph or Ar<sup>F</sup>) *via* [2+2] cycloaddition to form the azatitanacyclobutenes Ti(N<sub>2</sub><sup>R</sup>N<sup>Me</sup>){N{B(NAr'CH)<sub>2</sub>}C(H)C(Ar)}. In the case of R = Ar<sup>F</sup> these underwent subsequent intramolecular C–F bond cleavage/C–C coupling processes. Reaction of **11** and **21** with TolCCH also formed azatitanacyclobutenes, whereas Ar<sup>F</sup>CCH formed borylamide-acetylides *via* a C–H bond activation process which is endergonic in case of TolCCH. On heating, these kinetic products rearranged *via* alkyne elimination to form the corresponding azatitanacyclobutenes as the thermodynamic outcomes.

## TOC graphic



## Introduction

Group 4 organoimido (L)M(NR),<sup>1</sup> hydrazido (L)M(NNR<sub>2</sub>)<sup>2</sup> and alkylidene hydrazido/diazoalkane (L)M(NNCR<sub>2</sub>)<sup>3</sup> compounds (L = supporting ligand set; R = H or hydrocarbyl) have been extensively developed since the early 1990s. The dominant feature of these compounds is their addition or insertion reactions with unsaturated compounds at the M–N<sub>imide</sub> multiple bond. Less commonly, Group 4 imides can also activate the C–H bonds of organic substrates.<sup>11, 4</sup>

We have recently started to explore the chemistry of early transition metal borylimido compounds, (L)M(NBR<sub>2</sub>) (R = hydrocarbyl or heteroatom donor moiety) which are very underdeveloped, especially in terms of any reaction chemistry. The first examples reported were for Groups 5 and 6 by Wilkinson and Sundermeyer by the oxidative reaction of lower oxidation state precursors with N<sub>3</sub>BMes<sub>2</sub>.<sup>5</sup> Fryzuk *et al.* prepared a ditantalum borylimide by reaction of 9-BBN with a dinitrogen compound.<sup>6</sup> The first Group 4 borylimide was Mindiola's **1** (Fig. 1), synthesized from a parent imide ((L)Ti(NH)) with 2 equivs. of NaHBEt<sub>3</sub>.<sup>7</sup> We subsequently reported the similarly serendipitous formation of Cp\*Ti{MeC(N<sup>i</sup>Pr)<sub>2</sub>}(NBC<sub>8</sub>H<sub>14</sub>) (**2**, Fig. 1)<sup>8</sup> *via* reductive N–NR<sub>2</sub> bond cleavage of Cp\*Ti{MeC(N<sup>i</sup>Pr)<sub>2</sub>}(NNR<sub>2</sub>) (R = Me or Ph) with 9-BBN. More recently a catechol-functionalized borylimide was reported, again by Mindiola by reaction of a metallated nitride.<sup>9</sup>

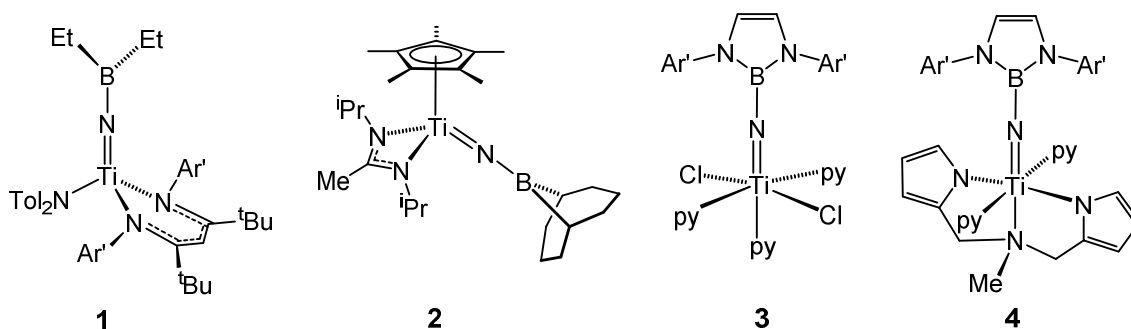


**Figure 1.** Examples of new titanium borylimido complexes. Ar' = 2,6-C<sub>6</sub>H<sub>3</sub><sup>i</sup>Pr<sub>2</sub>.<sup>7-8, 10</sup>

These routes are rather difficult to generalise, and in order to expand the synthetic potential of borylimido chemistry we have started to use the bulky borylamine<sup>11</sup> H<sub>2</sub>NB(NAr'CH)<sub>2</sub> (Ar' = 2,6-C<sub>6</sub>H<sub>3</sub><sup>i</sup>Pr<sub>2</sub>) as an entry point to both Group 3<sup>12</sup> and Group 4<sup>10</sup> derivatives. We very recently reported a number of titanium borylimides derived from H<sub>2</sub>NB(NAr'CH)<sub>2</sub>.<sup>10</sup> Of relevance to the work described below is the compound Ti{NB(NAr'CH)<sub>2</sub>}Cl<sub>2</sub>(py)<sub>3</sub> (**3**, Fig. 1) which we hoped would be able to act as an entry point to further derivatives of this type of borylimide. For example, reaction of **3** with a lithiated bis(pyrrolide)amine ligand, Li<sub>2</sub>N<sub>2</sub><sup>pyr</sup>N<sup>Me</sup>, gave **4** (Fig. 1). We have also reported a detailed bonding analysis of scandium<sup>12</sup> and titanium<sup>10</sup> borylimido compounds. In general these ligands are

more strongly  $\sigma$ -donating than their organoimido or hydrazido counterparts, with variable  $\pi$ -acceptor properties depending, as one would expect, on the nature of the substituents at boron.

In terms of reactivity, elegant contributions from Bettinger *et al.*,<sup>13</sup> as well as an early report from Paetzold,<sup>14</sup> have shown that the heteroatom-stabilized borylnitrenes  $B(N^iPr_2)_2$  and BCat (Cat = 1,2- $O_2C_6H_4$ ) can be photochemically generated from the corresponding azides  $X_2BN_3$  and undergo coupling reactions with CO and  $N_2$ , and insertion reactions into C–H, B–H, H–H and B–N bonds.<sup>13, 15</sup> To date, however, there has been only one report of the reactivity of a transition metal borylimido complex with small molecules.<sup>12</sup> We found that thermolysis of the methyl-borylamide  $(NacNac^{NMe_2})Sc(Me)\{NHB(NAr'CH)_2\}$  ( $NacNac^{NMe_2} = Ar'NC(Me)CHC(Me)NCH_2CH_2NMe_2$ ) generated the transient (not observed) borylimide  $(NacNac^{NMe_2})Sc\{NB(NAr'CH)_2\}$  *via* methane elimination. This imide underwent reversible  $sp^2$  C–H bond activation with pyridine or DMAP, and irreversible  $sp$  C–H bond activation or [2+2] cycloaddition with TolCCH and PhCCMe, respectively.

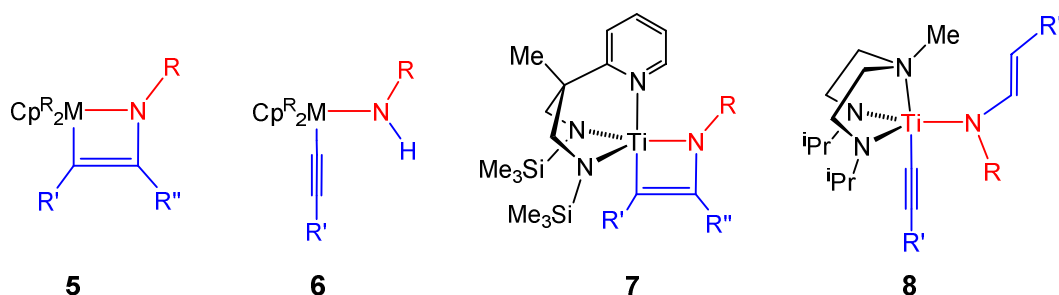


**Figure 2.** Examples of reaction products of organoimido and hydrazido compounds with alkynes ( $Cp^R = Cp$  or  $Cp^*$ ;  $R =$  alkyl, aryl or  $NNPh_2$ ).<sup>1b, 16</sup>

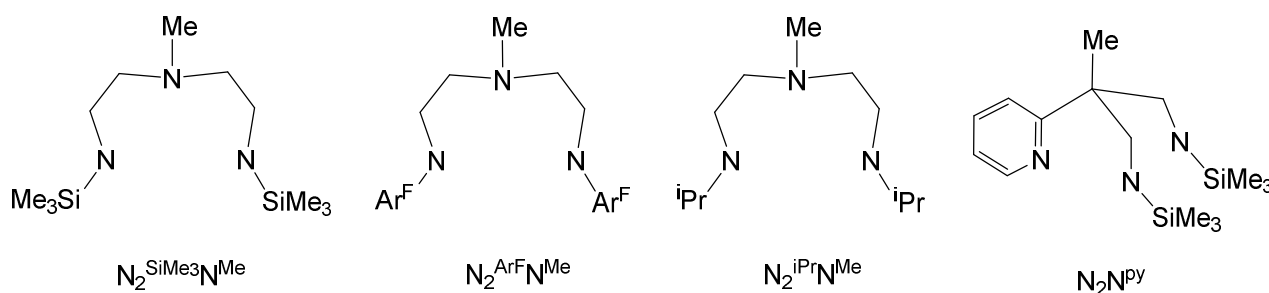
The stoichiometric and catalytic reactions of Group 4 organoimido and hydrazido compounds with alkynes been developed extensively for several decades, and principal landmarks in this area have been charted in recent reviews.<sup>1a-k, 2</sup> Internal alkynes and terminal alkynes  $R'C\equiv CR''$  ( $R' =$  hydrocarbyl;  $R'' =$  hydrocarbyl or H) typically undergo [2+2] cycloaddition at the  $M-N_{imide}$  multiple in either a 1,2 or 2,1 manner to give azametallacyclobutenes (*cf.* **5** and **7** in Fig. 2); such species can also be intermediates in the hydroamination or hydrohydrazination of alkynes.<sup>1b, 1h-j, 17</sup> Terminal alkynes can alternatively undergo C–H bond activation<sup>11</sup> *via* 1,2-addition across the  $M-N_{imide}$  bond (*cf.* **6** in Fig. 2) although this is relatively less common than the [2+2] cycloaddition pathway in general. Multiple C–H activation reactions can also occur, such as those forming the acetylide-vinylhydrazide compound **8**.<sup>16e</sup>

Given the historical and ongoing significance of the reactions of alkynes with organoimido and related metal-ligand multiply-bonded compounds, and the absence of any reactivity studies to date for Group 4 borylimido compounds, we decided to develop further aspects of this chemistry.

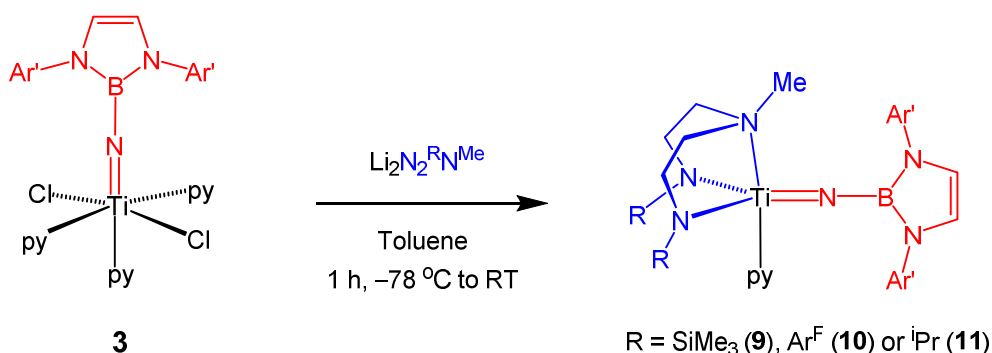
## Results and discussion

### Synthesis of diamide-amine supported borylimides

As described above,  $\text{Ti}\{\text{NB}(\text{NAr}'\text{CH})_2\}\text{Cl}_2(\text{py})_3$  (**3**), is a potentially useful starting material for the preparation of other new titanium borylimides, forming, for example,  $\text{Ti}(\text{N}_2^{\text{pyr}}\text{N}^{\text{Me}})\{\text{NB}(\text{NAr}'\text{CH})_2\}(\text{py})_2$  (**4**, Fig. 1) on reaction with  $\text{Li}_2\text{N}_2^{\text{pyr}}\text{N}^{\text{Me}}$ .<sup>10</sup> However, we found that the six-coordinate **4**, which features relatively weakly  $\pi$ -donating pyrrolide donors, does not undergo reactions with either terminal or internal alkynes. Based on our and others' reports of the diverse reactions of diamide-amine supported organoimido and related Group 4 compounds with alkynes (e.g. **7** and **8** in Fig. 2)<sup>1d, 16c, 18</sup> we therefore turned to the series of ligands  $\text{MeN}(\text{CH}_2\text{CH}_2\text{NR})_2$  ( $\text{N}_2^{\text{R}}\text{N}^{\text{Me}}$ ;  $\text{R} = \text{SiMe}_3$ ,  $\text{Ar}^{\text{F}}$  ( $\text{Ar}^{\text{F}} = \text{C}_6\text{F}_5$ ) or  $i\text{Pr}$ ) (2- $\text{C}_5\text{H}_4\text{N}$ ) $\text{CMe}(\text{CH}_2\text{NSiMe}_3)_2$  ( $\text{N}_2^{\text{N}^{\text{py}}}$ ). Strongly  $\pi$ -donating supporting ligands of this type generally lead to more reactive metal-ligand multiple bonds, while peripheral substitution can modulate reaction outcomes based on steric and electronic effects. We discuss first the synthesis and reactions of borylimides supported by the  $\text{MeN}(\text{CH}_2\text{CH}_2\text{NR})_2$  ligand family.



Reactions of **3** with the respective dilithiated ligands  $\text{Li}_2\text{N}_2^{\text{R}}\text{N}^{\text{Me}}$  in toluene at  $-78^\circ\text{C}$  gave the diamide-amine-supported borylimido compounds  $\text{Ti}(\text{N}_2^{\text{R}}\text{N}^{\text{Me}})\{\text{NB}(\text{NAr}'\text{CH})_2\}(\text{py})$  ( $\text{N}_2^{\text{R}}\text{N}^{\text{Me}} = \text{MeN}(\text{CH}_2\text{CH}_2\text{NR})_2$ ;  $\text{R} = \text{SiMe}_3$  (**9**),  $\text{Ar}^{\text{F}} = \text{C}_6\text{F}_5$  (**10**) or  $i\text{Pr}$  (**11**); Eq. 1) in 78 – 88 % isolated yield (the reactions are quantitative when followed on the NMR tube scale in  $\text{C}_6\text{D}_6$ ). Their  $^1\text{H}$  and  $^{13}\text{C}$  NMR spectra indicate that they have  $C_s$  symmetric structures in which the diamide-amine ligands are *fac*-coordinated, as well as containing a borylimido ligand and a pyridine donor.  $^{11}\text{B}$  resonances at 14.9 (**9**), 14.7 (**10**) and 15.2 (**11**) ppm fall within the range of *ca* 13 – 18 ppm we have previously found for borylimido complexes with the  $\text{NB}(\text{NAr}'\text{CH})_2$  moiety.<sup>10</sup>



### Equation 1

Diffraction-quality crystals of all three compounds were grown from hexane or pentane solutions. The molecular structure of **9** is shown in Fig. 3. Fig. S1 of the SI shows the structures of **10** and **11**. Selected bond lengths and angles for all three are given in Table 1. The three borylimido complexes all have trigonal-bipyramidal geometries, in which the diamide-amine ligands coordinate facially, and the borylimido ligands occupy an equatorial site *cis* to the axial NMe donor. The positioning of the titanium–nitrogen multiple bond in such complexes depends on both steric and electronic considerations. The electronic preference is for the multiple bond to be oriented axially (termed the *trans* arrangement), as when it is oriented in the equatorial site (termed the *cis* arrangement), the  $\pi$ -donor components of the Ti–N<sub>imide</sub> triple bond compete more with the N<sub>amide</sub> lone pairs for  $\pi$ -acceptor orbitals on the metal center.<sup>19</sup> In compounds **9**, **10** and **11**, steric demands clearly dominate, placing the borylimido ligand *cis* to the NMe donor. In all three structures, the boryl moiety is oriented such that the boryl ring lies nearly coplanar with the N(4)–Ti(1)–N(7) axis, this presumably being to avoid steric clash between the bulky Ar' groups and the N<sub>2</sub><sup>R</sup>N<sup>Me</sup> ligand substituents.

The Ti–N<sub>imide</sub> distances in the range 1.730(2) – 1.760(2) Å and nearly linear Ti–N<sub>imide</sub>–B angles in the range 160.05(10) – 170.38(18)° establish *sp* hybridisation at N<sub>imide</sub> and suggest Ti–N<sub>imide</sub> triple bonds in all three cases, in line with our previous MO analyses.<sup>10, 12</sup> The Ti–N<sub>amide</sub> distances are at the long end of usual range for titanium imido and related compounds in general.<sup>20</sup> Approximately trigonal planar geometries at the  $\pi$ -donor amide nitrogens (N<sub>amide</sub>) are indicated by the sums of the angles subtended at N<sub>amide</sub> being *ca.* 360°. The Ti–N<sub>py</sub> bond lengths in the range 2.2040(11) – 2.219(3) Å are typical.<sup>20</sup> The different N<sub>2</sub><sup>R</sup>N ligand amide substituents R in **9** – **11** give rise to differences in the Ti–N<sub>amide</sub> and Ti–N<sub>imide</sub> bond lengths. The shortest Ti–N<sub>imide</sub> and longest Ti–N<sub>amide</sub> distances are observed in **10** (R = C<sub>6</sub>F<sub>5</sub>) due to reduced N<sub>amide</sub>(2p)→Ti(3d)  $\pi$ -donation; the *iso*-propyl amide substituents in **11** on the other hand tend toward the shortest Ti–N<sub>amide</sub> and longer Ti–N<sub>imide</sub> bond lengths. The N<sub>imide</sub>–B bond lengths are equivalent within error.

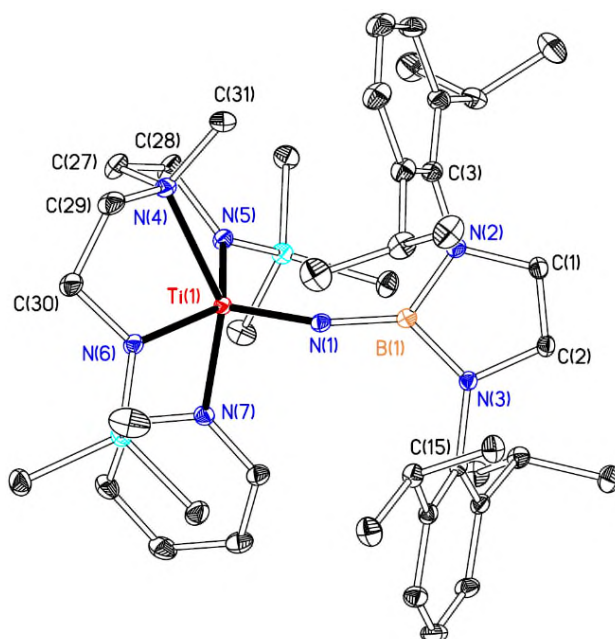


**Figure 3.** Displacement ellipsoid plot (20% probability) of  $\text{Ti}(\text{N}_2^{\text{SiMe}_3\text{N}^{\text{Me}}})\{\text{NB}(\text{NAr}'\text{CH})_2\}(\text{py})$  (**9**). H atoms are omitted for clarity.

**Table 1.** Selected bond lengths (Å) and angles (°) for  $\text{Ti}(\text{N}_2^{\text{R}^{\text{N}^{\text{Me}}}})\{\text{NB}(\text{NAr}'\text{CH})_2\}(\text{py})$  (R = SiMe<sub>3</sub> (**9**,  $\tau = 0.17$ ), Ar<sup>F</sup> (**10**,  $\tau = 0.37$ ) or <sup>i</sup>Pr (**11**,  $\tau = 0.46$ )).

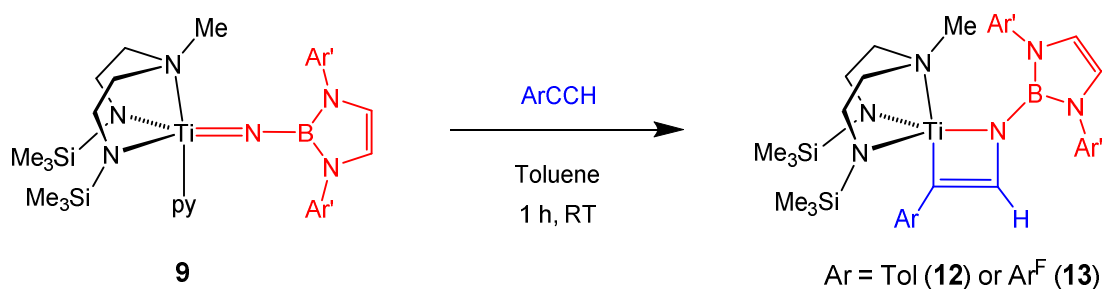
	<b>9</b>	<b>10</b>	<b>11</b>
Ti(1)–N(1)	1.7537(12)	1.730(2)	1.760(2)
Ti(1)–N(5)	2.0193(12)	2.047(2)	1.998(3)
Ti(1)–N(6)	2.0278(12)	2.015(2)	1.974(3)
Ti(1)–N(4)	2.2577(11)	2.2279(19)	2.245(3)
Ti(1)–N(7)	2.2040(11)	2.2042(19)	2.219(3)
N(1)–B(1)	1.4190(19)	1.418(3)	1.417(4)
Ti(1)–N(1)–B(1)	160.05(10)	170.38(18)	169.9(2)

### Reactions of diamide-amine supported borylimides with alkynes

As mentioned, one aim of this work was to study the reactions of this class of borylimido compounds with selected representative alkynes. Whereas  $\text{Ti}(\text{N}_2^{\text{pyr}^{\text{N}^{\text{Me}}}})\{\text{NB}(\text{NAr}'\text{CH})_2\}(\text{py})_2$  (**4**) showed no reactivity with terminal or internal alkynes, the diamide-amine supported compounds **9** – **11** reacted with the terminal alkynes TolCCH (Tol = 4-C<sub>6</sub>H<sub>4</sub>Me) and Ar<sup>F</sup>CCH (chosen for their differing acidity) giving different kinetic and/or thermodynamic products, depending on the  $\text{N}_2^{\text{R}^{\text{N}^{\text{Me}}}}$  supporting ligand. In contrast, the more electron-rich and sterically hindered, internal alkynes

PhCCMe and MeCCMe did not react with any of the borylimides reported here. We discuss the reactions of **9**, **10** and **11** in turn.

*Reactions of  $Ti(N_2^{SiMe_3}N^{Me})\{NB(NAr'CH)_2\}(py)$  (**9**).* Reactions of  $Ti(N_2^{SiMe_3}N^{Me})\{NB(NAr'CH)_2\}(py)$  (**9**) with TolCCH or  $Ar^FCCH$  were both quantitative on the NMR tube scale, forming the azatitanacyclobutene complexes  $Ti(N_2^{SiMe_3}N^{Me})\{N\{B(NAr'CH)_2\}C(H)C(Ar)\}$  ( $Ar = Tol$  (**12**) or  $Ar^F$  (**13**)). The reactions were rapid at room temperature (RT), with immediate color changes from red to red-black being observed in both cases. On the preparative scale **12** and **13** were isolated as waxy solids in 68 and 66% yield, respectively (Eq. 2).



**Equation 2**

The assignment of **12** and **13** as azatitanacyclobutenes, formed by [2+2] cycloaddition of the alkyne is consistent with their NMR and IR data and the X-ray structure of **12**. The  $^1H$  NMR spectra show singlets (1 H intensity) at characteristic chemical shifts of 10.51 and 10.43 for the C=CH of the azatitanacyclobutene unit. The  $^{11}B$  NMR resonances (23.8 and 23.4 ppm, respectively) are consistent with borylamide groups,<sup>8, 10, 12</sup> and are shifted significantly from the value of 14.9 ppm in **9**. The anti-Markovnikov (AM) type regiochemistry (so-called because this is the isomer that would give rise to that hydroamination product upon protolysis) of the [2+2] cycloaddition was established from HSQC and HMBC  $^1H$ - $^{13}C$  NMR spectra. The electronic origins of the AM regioselectivity of [2+2] cycloaddition in these types of diamide-amine system (e.g. as for **7** in Fig. 2) has been accounted for using DFT calculations on related metallacyclic complexes  $Ti(N_2N^L)\{NRC(H)C(Ar)\}$  ( $N_2N^L = N_2^{SiMe_3}N^{Me}$  or  $N_2N^{py}$ ). Positioning of the aryl ring on the Ti-bound carbon stabilizes the negative charge which builds up at this point in the azatitanacyclobutene ring.<sup>16d</sup> Density Functional Theory (DFT) calculations described below on homologous model [2+2] cycloaddition reaction products likewise found an electronic preference for AM type cycloaddition of between 3.5 and 7.4 kcal mol<sup>-1</sup> for PhCCH and  $Ar^FCCH$ , respectively.

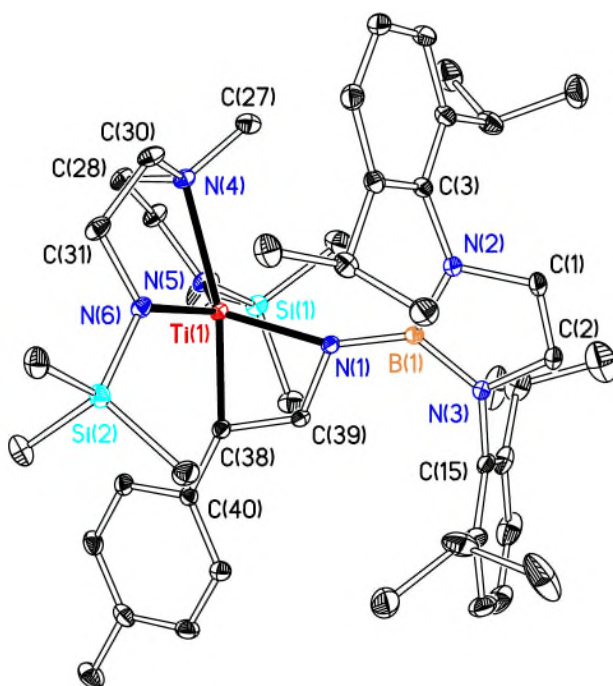


**Figure 4.** Displacement ellipsoid plot (25% probability) of  $\text{Ti}(\text{N}_2^{\text{SiMe}_3}\text{N}^{\text{Me}})\{\text{N}\{\text{B}(\text{NAr}'\text{CH})_2\}\text{C}(\text{H})\text{C}(\text{Tol})\}$  (**12**). H atoms are omitted for clarity. Selected bond distances (Å) and angles (°): Ti(1)–N(1) 1.9784(10), Ti(1)–N(4) 2.2900(10), Ti(1)–N(5) 1.9798(10), Ti(1)–N(6) 1.9880(10), Ti(1)–C(38) 2.0026(12), N(1)–B(1) 1.4275(16), N(1)–C(39) 1.4277(14), C(38)–C(39) 1.3715(16), N(1)–Ti(1)–C(38) 75.52(4), Ti(1)–N(1)–B(1) 157.51(8), Ti(1)–C(38)–C(39) 81.22(7), N(1)–C(39)–C(38) 121.12(10) ( $\tau = 0.59$ ).

The solid state structure of **12** as determined by X-ray diffraction is shown in Figure 4, along with selected bond distances and angles. Compound **12** has a distorted pentacoordinate geometry, having an Addison  $\tau$  value<sup>21</sup> of 0.59 (for an ideal square-based pyramid,  $\tau = 0$ ; for a trigonal bipyramid,  $\tau = 1$ ). The diamide-amine ligand remains facially coordinated to the metal, and the  $\kappa^2$ -coordination of the C(38)–C(39)–N(1) unit to form the four-membered azatitanacyclobutene ring with Ti(1) is also confirmed. The C(38)–C(39) bond length of 1.3715(16) Å indicates a carbon–carbon double bond, and the Ti(1)–N(1) and Ti(1)–C(38) bond lengths of 1.9784(10) and 2.0026(12) Å respectively are consistent with  $sp^2$ -type single bonds being formed to the metal center. Several analogues of **12** and **13** with diamide-amine ligands have been structurally characterised for organoimido and hydrazido systems.<sup>20</sup> However, these are only the second examples of such azametallacycles formed for a borylimide, the first being  $(\text{NacNac}^{\text{NMe}_2})\text{Sc}\{\text{N}\{\text{B}(\text{NAr}'\text{CH})_2\}\text{C}(\text{Me})\text{C}(\text{Ph})\}$ , formed from  $\text{PhCCMe}$  and a transient scandium borylimide generated from  $(\text{NacNac}^{\text{NMe}_2})\text{Sc}(\text{Me})\{\text{NHB}(\text{NAr}'\text{CH})_2\}$  by methane elimination under thermolytic conditions.<sup>12</sup>

A competition experiment in  $\text{C}_6\text{D}_6$  was also carried out between **9** and five equivs. of  $\text{TolCCH}$  and of  $\text{Ar}^{\text{F}}\text{CCH}$  at room temperature, resulting in a *ca.* 2:1 molar ratio mixture of **12** and **13** which did not

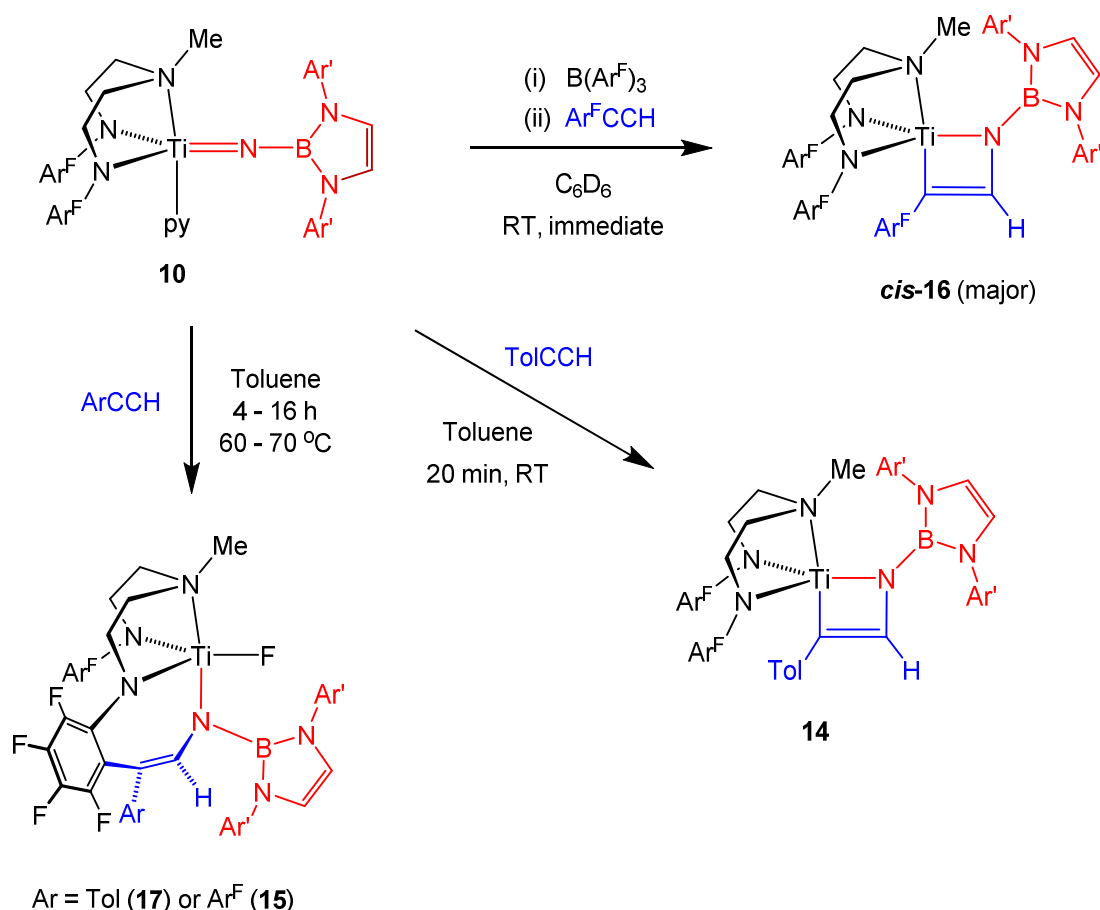


change with time or upon heating the mixtures further. The formation of a larger proportion of **12** is interesting since previous experimental and DFT have shown that related metallacyclic species are more stable when bearing electron-withdrawing substituents.<sup>16d, 18e, f, 22</sup> DFT calculations (Table 2) were therefore carried out to assess the thermodynamic preferences for forming **12** and **13**. These found that  $\Delta_r G_{298}$  for the formation of **12** + py from **9** + TolCCH was 5.6 kcal mol<sup>-1</sup> less exergonic than the corresponding reaction with Ar<sup>F</sup>CCH to form **13** + py. Together, these experimental and DFT results show that metallacycle formation in this system is under kinetic rather than thermodynamic control, and imply that the barrier to retrocyclization is inaccessible under these reaction conditions. The DFT results (Table 2) also suggest that a C–H bond activation product between Ar<sup>F</sup>CCH and **9** might be thermodynamically accessible, although the computed  $\Delta_r G_{298}$  value of -0.3 kcal mol<sup>-1</sup> for this reaction is outside the precision of DFT theory at this level, and C–H activation products were not observed with **9** and ArCCH. Further experimental and DFT studies concerning these mechanisms are discussed later on.

*Reactions of  $Ti(N_2^{Ar^F}N^{Me})\{NB(NAr'CH)_2\}(py)$  (**10**).* On the NMR tube scale in C<sub>6</sub>D<sub>6</sub>, the reaction of **10** with TolCCH at room temperature gave immediate, quantitative conversion to a single [2+2] cycloaddition product  $Ti(N_2^{Ar^F}N^{Me})\{N\{B(NAr'CH)_2\}C(H)C(Tol)\}$  (**14**) at RT. Compound **14** was subsequently isolated as a deep red solid in 76% yield (Scheme 1) on the preparative scale. The X-ray structure of **14** (Fig. S2 of the SI) confirms the AM type regiochemistry depicted in Scheme 1, which is supported by the other spectroscopic and analytical data. Molecules of **14** have an analogous structure to that of **12** (Fig. 4), possessing a distorted pentacoordinate geometry ( $\tau = 0.69$ ) at titanium. They also feature intramolecular offset face-to-face<sup>23</sup>  $\pi$ -interactions between the one of the amide-bound Ar<sup>F</sup> rings of the N<sub>2</sub><sup>Ar<sup>F</sup></sup>N<sup>Me</sup> ligand and the ring carbons of the tolyl group derived from the TolCCH substrate (av. interplanar spacing *ca.* 3.4 Å) as discussed further below.

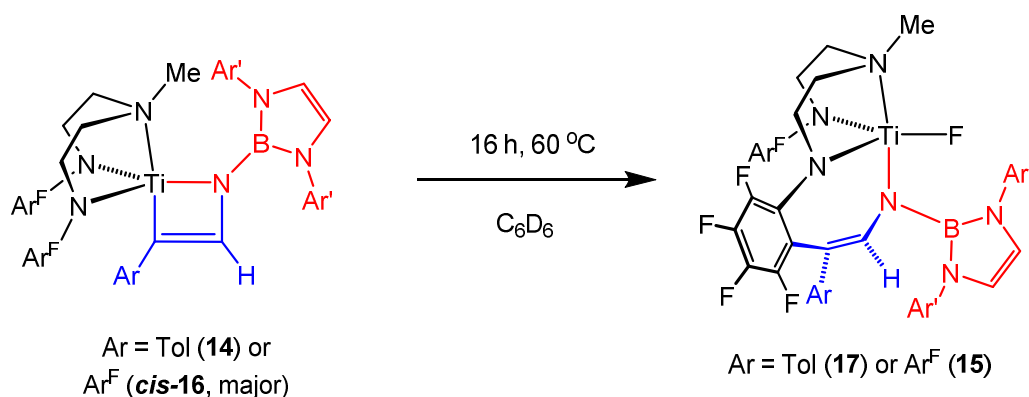
**Table 2.** DFT computed Gibbs free energies ( $\Delta_r G$  kcal mol<sup>-1</sup> at 298 K (343 K in brackets)) for selected reactions of Ti(N<sub>2</sub><sup>R</sup>N<sup>Me</sup>){NB(NAr'CH)<sub>2</sub>}(py) (R = SiMe<sub>3</sub> (**9**), Ar<sup>F</sup> (**10**) or <sup>i</sup>Pr (**11**)) or Ti(N<sub>2</sub>N<sup>Py</sup>){NB(NAr'CH)<sub>2</sub>}(py) (**21**) with alkynes. In the case of **11** the data are for the *cis* isomer product for ease of comparison.

Imido compound	Alkyne	Reaction type	$\Delta_r G$ (kcal mol <sup>-1</sup> )
Ti(N <sub>2</sub> <sup>SiMe<sub>3</sub></sup> N <sup>Me</sup> ){NB(NAr'CH) <sub>2</sub> }(py) ( <b>9</b> )	TolCCH	cycloaddition	-7.0
Ti(N <sub>2</sub> <sup>SiMe<sub>3</sub></sup> N <sup>Me</sup> ){NB(NAr'CH) <sub>2</sub> }(py) ( <b>9</b> )	Ar <sup>F</sup> CCH	cycloaddition	-12.6
Ti(N <sub>2</sub> <sup>SiMe<sub>3</sub></sup> N <sup>Me</sup> ){NB(NAr'CH) <sub>2</sub> }(py) ( <b>9</b> )	TolCCH	C–H activation	2.8
Ti(N <sub>2</sub> <sup>SiMe<sub>3</sub></sup> N <sup>Me</sup> ){NB(NAr'CH) <sub>2</sub> }(py) ( <b>9</b> )	Ar <sup>F</sup> CCH	C–H activation	-0.3
Ti(N <sub>2</sub> <sup>Ar<sup>F</sup></sup> N <sup>Me</sup> ){NB(NAr'CH) <sub>2</sub> }(py) ( <b>10</b> )	TolCCH	cycloaddition	-11.4
Ti(N <sub>2</sub> <sup>Ar<sup>F</sup></sup> N <sup>Me</sup> ){NB(NAr'CH) <sub>2</sub> }(py) ( <b>10</b> )	Ar <sup>F</sup> CCH	cycloaddition	-9.9
Ti(N <sub>2</sub> <sup>iPr</sup> N <sup>Me</sup> ){NB(NAr'CH) <sub>2</sub> }(py) ( <b>11</b> )	TolCCH	cycloaddition	-11.6
Ti(N <sub>2</sub> <sup>iPr</sup> N <sup>Me</sup> ){NB(NAr'CH) <sub>2</sub> }(py) ( <b>11</b> )	Ar <sup>F</sup> CCH	cycloaddition	-13.6
Ti(N <sub>2</sub> <sup>iPr</sup> N <sup>Me</sup> ){NB(NAr'CH) <sub>2</sub> }(py) ( <b>11</b> )	TolCCH	C–H activation	0.3
Ti(N <sub>2</sub> <sup>iPr</sup> N <sup>Me</sup> ){NB(NAr'CH) <sub>2</sub> }(py) ( <b>11</b> )	Ar <sup>F</sup> CCH	C–H activation	-2.4
Ti(N <sub>2</sub> N <sup>Py</sup> ){NB(NAr'CH) <sub>2</sub> }(py) ( <b>21</b> )	TolCCH	cycloaddition	-10.2 [10.3]
Ti(N <sub>2</sub> N <sup>Py</sup> ){NB(NAr'CH) <sub>2</sub> }(py) ( <b>21</b> )	Ar <sup>F</sup> CCH	cycloaddition	-15.0 [-14.7]
Ti(N <sub>2</sub> N <sup>Py</sup> ){NB(NAr'CH) <sub>2</sub> }(py) ( <b>21</b> )	TolCCH	C–H activation	1.3 [1.5]
Ti(N <sub>2</sub> N <sup>Py</sup> ){NB(NAr'CH) <sub>2</sub> }(py) ( <b>21</b> )	Ar <sup>F</sup> CCH	C–H activation	-3.9 [-3.9]
Ti(N <sub>2</sub> N <sup>Py</sup> ){NB(NAr'CH) <sub>2</sub> }(py) ( <b>21</b> )	Ar <sup>F</sup> CCD	C–D activation	-4.0 [-4.0]
Ti(N <sub>2</sub> N <sup>Py</sup> ){NB(NAr'CH) <sub>2</sub> }(py) ( <b>21</b> )	PhCCMe	cycloaddition	1.7 [2.3]
Ti(N <sub>2</sub> N <sup>Py</sup> ){NB(NAr'CH) <sub>2</sub> }(py) ( <b>21</b> )	MeCCMe	cycloaddition	5.8 [5.9]



**Scheme 1.** Reactions of  $\text{Ti}(\text{N}_2^{\text{Ar}^{\text{F}}\text{N}^{\text{Me}}})\{\text{NB}(\text{NAr}'\text{CH})_2\}(\text{py})$  (**10**) with  $\text{ArCCH}$ . Minor (*trans*) isomer of **16** omitted for clarity.

The NMR tube scale reaction between **10** and  $\text{Ar}^{\text{F}}\text{CCH}$  was slower than for  $\text{TolCCH}$ , and in this case two products (**15** and **16**) were found to concurrently form. Heating the mixture at  $70^\circ\text{C}$  resulted in quantitative conversion of **10** and  $\text{Ar}^{\text{F}}\text{CCH}$  exclusively to **15** which was isolated as a yellow-orange solid in 57% yield (Scheme 1) after scale-up. Crystallographic characterization (*vide infra*) showed that this compound was the titanium fluoride complex,  $\text{Ti}\{\text{MeN}(\text{CH}_2\text{CH}_2\text{NAr}^{\text{F}})\{\text{CH}_2\text{CH}_2\text{NC}_6\text{F}_4\text{C}(\text{Ar}^{\text{F}})\text{CHNB}(\text{NAr}'\text{CH})_2\}\}(\text{F})$  (**15**), in which one of the  $\text{C}_6\text{F}_5$  rings of the supporting ligand has become coupled to a vinyl-borylamide moiety to form a seven-membered metallacycle, accompanied by migration of a fluorine from one of the  $\text{Ar}^{\text{F}}$  rings of the  $\text{N}_2^{\text{Ar}^{\text{F}}\text{N}^{\text{Me}}}$  ligand to the titanium center. Compound **14**, also underwent conversion to a titanium fluoride complex, namely  $\text{Ti}\{\text{MeN}(\text{CH}_2\text{CH}_2\text{NAr}^{\text{F}})\{\text{CH}_2\text{CH}_2\text{NC}_6\text{F}_4\text{C}(\text{Tol})\text{CHNB}(\text{NAr}'\text{CH})_2\}\}(\text{F})$  (**17**) upon heating in  $\text{C}_6\text{D}_6$  at  $60^\circ\text{C}$  (Eq. 3). This compound is structurally analogous to **15**. On the preparative scale, **17** was more conveniently prepared in a one-pot manner directly from **10** and  $\text{TolCCH}$  at  $70^\circ\text{C}$  for 3.5 h, resulting giving the product a yellow-orange solid in 47% yield.



### Equation 3

Compound **16** was identified as the AM-type [2+2] cycloaddition product  $\text{Ti}(\text{N}_2^{\text{Ar}^{\text{F}}}\text{N}^{\text{Me}})\{\text{N}\{\text{B}(\text{NAr}'\text{CH})_2\}\text{C}(\text{H})\text{C}(\text{Ar}^{\text{F}})\}$ , which is an intermediate in the formation of **15**. The sole formation of **16** could be achieved on the NMR tube scale by addition of 1 equiv.  $\text{B}(\text{Ar}^{\text{F}})_3$  (as a trapping agent for the eliminated py, forming  $\text{B}(\text{Ar}^{\text{F}})_3(\text{py})^{18\text{e}}$ ), and was characterised *in situ* by NMR spectroscopy as a mixture of two isomers (3:1 ratio), with the NB atom of the AM-type metallacycle being positioned either *cis* to the apical NMe donor of the  $\text{N}_2^{\text{Ar}^{\text{F}}}\text{N}^{\text{Me}}$  ligand (as shown in Scheme 1) or *trans*. Analogues of both *cis*- and *trans*-**16** have been reported previously.<sup>16b</sup>

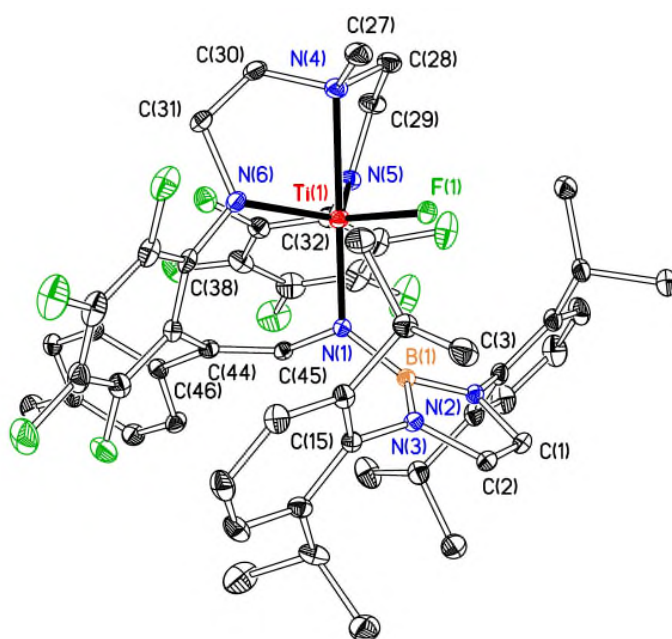


**Figure 5.** Displacement ellipsoid plot (20% probability) of  $\text{Ti}\{\text{MeN}(\text{CH}_2\text{CH}_2\text{NAr}^{\text{F}})\{\text{CH}_2\text{CH}_2\text{NC}_6\text{F}_4\text{C}(\text{Tol})\text{CHNB}(\text{NAr}'\text{CH})_2\}\}(\text{F})$  (**17**). H atoms are omitted for clarity. Selected bond lengths (Å) and angles (°): Ti(1)–N(1) 1.9105(17), Ti(1)–N(4) 2.265(2), Ti(1)–N(5) 1.957(2), Ti(1)–N(6) 1.936(2), Ti(1)–F(1) 1.8226(13), N(1)–B(1) 1.470(3), N(1)–C(45) 1.404(3), C(44)–C(45) 1.353(3), Ti(1)–N(1)–B(1) 125.08(14) ( $\tau = 0.95$ ).

The titanium fluoride complexes **15** and **17** were crystallographically characterised. The solid state structures are shown in Fig. 5 and Fig. S3 of the SI, respectively, along with selected bond distances and angles. Both are five-coordinate with slightly distorted trigonal bipyramidal geometries ( $\tau = 0.93$  (**15**) and  $0.95$  (**17**)), in which the diamide-amine ligand is *fac*-coordinated. The fluoride ligand occupies an equatorial site, and the N-boryl group lies *trans* to the NMe donor in the opposing axial site. Both complexes incorporate a seven-membered metallacycle, formed from the coupling of a ligand  $C_6F_5$  group onto what was the Ti-bound carbon in the azatitanacyclobutenes **16** and **14**. The olefinic C=C bonds have distances of  $1.343(3)$  and  $1.353(3)$  Å in **15** and **17** respectively, so are significantly shorter than the C=C bond distance in the solid state structure of **14** ( $1.389(2)$  Å). Meanwhile, the C–C and C–N bond distances either side of the olefinic linkage are consistent with being single bonds. The NMR data for **15** and **17** are consistent with  $C_1$ -symmetric complexes. Of particular note are singlets of intensity 1 H at 6.72 and 6.59 ppm for the vinylic groups  $ArC=C(H)-N$  in the  $^1H$  NMR spectrum, and singlets at  $-100.0$  and  $-102.5$  ppm in the  $^{19}F$  NMR spectrum corresponding to Ti–F. The  $^{11}B$  NMR spectra showed resonances at 22.4 and 22.9 ppm, for **15** and **17**, respectively.

The mechanism of formation of **15** and **17** proceeds *via* initial cycloaddition of the alkyne to give the azatitanacyclobutenes **16** and **14**. It is proposed that nucleophilic attack of the Ti-bound carbon of the metallacycle unit on the *ortho* position of a supporting ligand  $C_6F_5$  ring takes place, resulting in an expanded, seven-membered metallacycle, and accompanied by migration of the displaced fluoride atom to the titanium center. Related examples of C–F bond activation in  $d^0$  Group 4 metal species have been reported.<sup>24</sup>

The reactions **14**  $\rightarrow$  **17** and **16**  $\rightarrow$  **15** were followed by  $^1H$  NMR spectroscopy in the temperature range 327 – 339 K. They followed first order kinetics as judged by the linear semi-logarithmic plots shown in Figs. S4 and S5 of the SI. An Eyring analysis of first order rate constants at the various temperatures (Tables S1 (for **14**  $\rightarrow$  **17**) and S2 (for **16**  $\rightarrow$  **15**) of the SI) gave the activation parameters  $\Delta H^\ddagger = 14.1(1.5)$  kcal mol $^{-1}$  and  $\Delta S^\ddagger = -34.3(4.4)$  cal mol $^{-1}$  K $^{-1}$  ( $\Delta G_{333}^\ddagger = 25.5(1.5)$  kcal mol $^{-1}$ ) for **14**. For the reaction of **16**, the activation parameters obtained were  $\Delta H^\ddagger = 13.9(1.0)$  kcal mol $^{-1}$  and  $\Delta S^\ddagger = -35.3(2.9)$  cal mol $^{-1}$  K $^{-1}$  ( $\Delta G_{333}^\ddagger = 25.7(1.0)$  kcal mol $^{-1}$ ). The negative entropies of activation are consistent with the proposed intramolecular mechanism, which is expected to proceed *via* a rather constrained transition state.

Interestingly, the activation parameters for both **14**  $\rightarrow$  **17** and for **16**  $\rightarrow$  **15** are very similar. Since one would expect the nucleophilicity of the metallacyclic carbons  $Ti-C(Ar)C(H)$  to differ more significantly between  $Ar = Tol$  and  $Ar = Ar^F$ , the data could imply that C–F bond cleavage as

opposed to C–C(Ar) bond formation is the main contributor to the rate-determining step of the reactions. Alternatively (or additionally), we also considered that the ground state stabilities of the metallacycles **14** and **16** themselves may differ because of the different possible  $\pi$ -interactions between the Ar<sup>F</sup> ring of the N<sub>2</sub><sup>Ar<sup>F</sup></sup>N<sup>Me</sup> supporting ligand and the metallacycle Ar group (Ar = Ph or Ar<sup>F</sup>). The importance of non-covalent interactions between hydrogen-substituted arene rings in supramolecular chemistry is of course well-established.<sup>25</sup> Arene–perfluoroarene interactions, however, represent a special case. For examples, calculations have suggested that the interactions between C<sub>6</sub>H<sub>6</sub> and C<sub>6</sub>F<sub>6</sub> (as in the 1:1 benzene–perfluorobenzene complex<sup>26</sup> which has a melting point of 24 °C) can be up to *ca.* 5 kcal mol<sup>–1</sup> more favorable than between either of the two types of ring (i.e., C<sub>6</sub>H<sub>6</sub> or C<sub>6</sub>F<sub>6</sub>) alone.<sup>27</sup>

To explore this further we computed the DFT structure of both **14** (based on the crystallographically determined structure) and *cis*-**16**. As in the X-ray structure of **14**, the computed geometries feature  $\pi$ -interactions between the metallacycle aryl ring and one of the amido Ar<sup>F</sup> groups, giving an average interplanar spacing *ca.* 3.2 Å in each case which is comparable to the value of 3.4 Å found experimentally for **14**. Importantly, the computed  $\Delta_rG$  for formation of **14** (Table 2) was 1.5 kcal mol<sup>–1</sup> *more* exergonic than for **16**. As mentioned, it has previously been found that electron-withdrawing groups stabilise metallacycles of the type present in **14** and **16** (*cf.* Table 2 for the reactions of **9** – **11** and **21** with ArCCH (Ar = Ph or Ar<sup>F</sup>) and DFT calculations discussed below for model systems). The increased stability of **14** is attributed to the more favorable  $\pi$ -interactions expected between fluorine-substituted and –non-substituted arene rings. It seems likely (based also on the transition state for the [2+2] cycloaddition for model systems, discussed later on) that the faster rate of reaction of reaction of **10** with TolCCH might be attributed to similar favorable  $\pi$ -interactions in the transition state leading to **14**; likewise the similar reaction rates for **14** → **17** and **16** → **15** would seem attributable, at least in part, to the same effect.

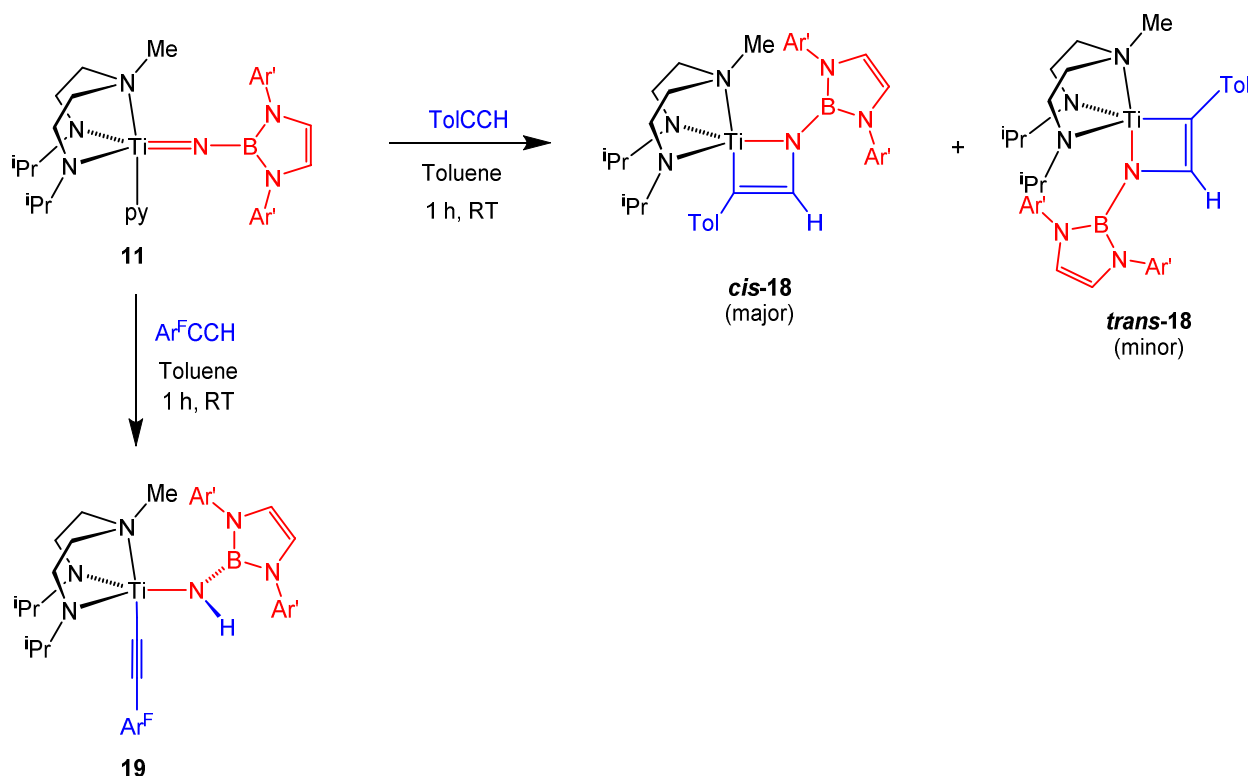
*Reactions of Ti(N<sub>2</sub><sup>iPr</sup>N<sup>Me</sup>){NB(NAr'CH)<sub>2</sub>}(py) (**11**).* In our previous studies of titanium hydrazide chemistry we found that the sterically more open *iso*-propyl amide compound Ti(N<sub>2</sub><sup>iPr</sup>N<sup>Me</sup>)(NNPh<sub>2</sub>)(py) gave the acetylide-vinylamide compound **8** (Fig. 2) incorporating two equivs. of terminal alkyne,<sup>16e</sup> *via* a (non-observed) metallacyclic intermediate. It was therefore of interest to explore the reactions of the borylimide **11** with alkynes. NMR tube scale reactions showed no reactivity with internal alkynes, despite the lower steric demands and higher activating ability of the *iso*-propyl amide supporting ligand. The reactions with TolCCH and Ar<sup>F</sup>CCH are shown in Scheme 2.

Addition of TolCCH to a solution of **11** in C<sub>6</sub>D<sub>6</sub> gave an immediate color change to deep red-brown, and quantitative conversion to a [2+2] cycloaddition product **18**. In contrast, use of Ar<sup>F</sup>CCH resulted in an instantaneous color change to orange, with the <sup>1</sup>H NMR spectrum indicating quantitative conversion to a borylamide-acetylide compound **19** via C–H bond activation of the alkyne. On the preparative scale, Ti(N<sub>2</sub><sup>i</sup>PrN<sup>Me</sup>){N{B(NAr'CH)<sub>2</sub>}C(H)C(Tol)} (**18**) and Ti(N<sub>2</sub><sup>i</sup>PrN<sup>Me</sup>){NHB(NAr'CH)<sub>2</sub>}(CCAr<sup>F</sup>) (**19**), were isolated in 43 and 51% yields, respectively (Scheme 2), the modest isolated yields being due to the high solubility of these compounds. No further reactions of **18** or **19** were observed with an excess of either alkyne.

The <sup>1</sup>H NMR spectrum of **18** is consistent with this being a mixture of two isomeric forms of an azatitanacyclobutene complex in a *ca* 3:1 ratio as illustrated. Two singlets (1 H intensity) are observed at 10.32 and 9.35 ppm for the metallacycle moiety, corresponding to the major and minor isomer, respectively. HSQC and HMBC correlations confirm that both isomers have anti-Markovnikov type regiochemistry. The <sup>11</sup>B spectrum shows a single (overlapping) resonance for the two isomer at 22.1 ppm (*cf. ca.* 22 – 23.5 ppm in the metallacycles **12** – **14** and *cis*-**16**). A <sup>1</sup>H–<sup>1</sup>H ROESY NMR experiment established *cis*-**18** (analogous to **12** – **14** and *cis*-**16**) as the major isomer. The accessibility of the *trans*-**18** isomer is attributed to the reduced steric demands of the *iso*-propyl substituents. Note that the acetylide-vinylamide compound **8** (Fig. 1) also exists as a mixture of *cis* and *trans* isomers,<sup>16c</sup> as do reaction products of Ti(N<sub>2</sub><sup>i</sup>PrN<sup>Me</sup>)(NNPh<sub>2</sub>)(py) with other substrates.<sup>8a</sup> In addition, whereas Ti(N<sub>2</sub>N<sup>py</sup>)(NAr')(py) reacted with PhCCH forming a metallacyclic product analogous to *cis*-**18**, the same reaction with Ti(N<sub>2</sub>N<sup>py</sup>)(N<sup>t</sup>Bu)(py) formed an analogues of *trans*-**18**.<sup>16b</sup> Diffraction-quality crystals of **18** (as the *cis* isomer) were grown from hexane. The molecular structure is shown in Fig. S6 of the SI, along with selected bond distances and angles. Molecules of *cis*-**18** have an analogous structure to those of **12** and **14**, having an overall pentacoordinate geometry ( $\tau = 0.58$  and 0.63 for the two crystallographically independent molecules).

The <sup>1</sup>H and <sup>13</sup>C NMR spectra of **19** indicate a single isomer with C<sub>s</sub> symmetry. A slightly broadened singlet (1 H intensity) is observed at 6.58 ppm, this being assigned as the borylamide ligand NH. The <sup>11</sup>B resonance at 23.0 ppm (*cf.* 14.7 - 15.2 in the imides **9** – **11**) is indicative of a borylamide ligand. A very similar <sup>11</sup>B shift (22.9 ppm) was found for the scandium borylamide-acetylide (NacNac<sup>NMe<sub>2</sub></sup>)Sc{NHB(NAr'CH)<sub>2</sub>}(CCTol) formed from transient (NacNac<sup>NMe<sub>2</sub></sup>)Sc{NB(NAr'CH)<sub>2</sub>} and TolCCH.<sup>12</sup> These data rule out an alternative structure where this H atom is bound to an N<sub>amide</sub> atom of the diamide-amine supporting ligand. In the <sup>13</sup>C NMR spectrum, the two acetylide carbons (TiCCAr<sup>F</sup>) are assigned at 162.0 and 83.7 ppm, corresponding to the carbon directly bonded to Ti, and the one adjacent to the Ar<sup>F</sup> ring, respectively. Additionally, a band at 2094 cm<sup>-1</sup> (DFT: 2108 cm<sup>-1</sup>

<sup>1</sup>) in the IR spectrum of **19** is attributed to  $\nu(\text{C}\equiv\text{C})$ , which is consistent with titanium amide-acetylide or hydroxide-acetylide compounds reported previously.<sup>16a, 28</sup>



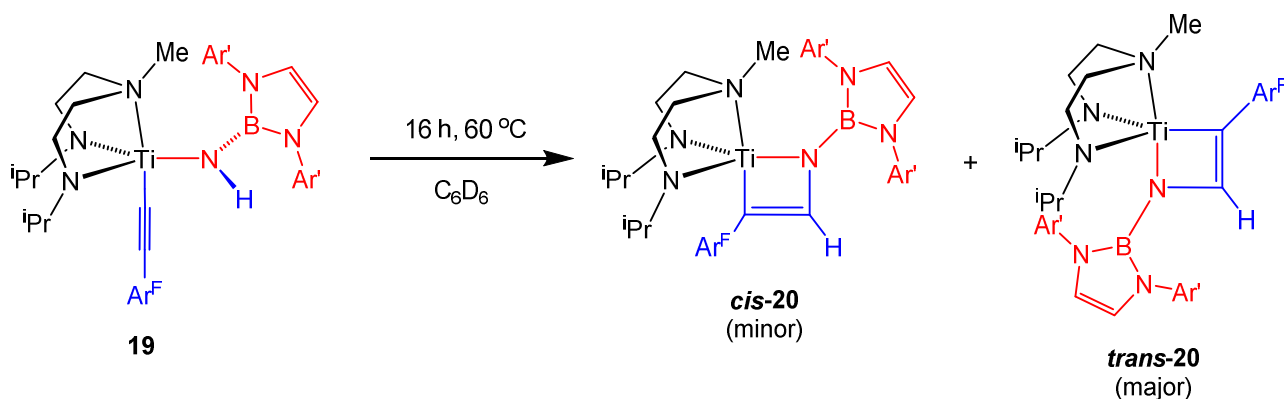
**Scheme 2.** Reactions of  $\text{Ti}(\text{N}_2^{\text{iPr}}\text{N}^{\text{Me}})\{\text{NB}(\text{NAr}'\text{CH})_2\}(\text{py})$  (**11**) with TolCCH and  $\text{Ar}^{\text{F}}\text{CCH}$ .

The divergent behavior of **11** with TolCCH and  $\text{Ar}^{\text{F}}\text{CCH}$  warranted further investigation. DFT calculations on the thermodynamic preferences ( $\Delta_{\text{r}}G$  values) of **11** and  $\text{ArCCH}$  for cycloaddition vs C–H bond activation (Table 2) showed that formation of **19** (and py) was exergonic ( $\Delta_{\text{r}}G = -2.4 \text{ kcal mol}^{-1}$ ). The corresponding reaction for TolCCH was slightly endergonic ( $\Delta_{\text{r}}G = 0.3 \text{ kcal mol}^{-1}$ ) whereas cycloaddition (forming **cis-18**) was substantially exergonic ( $\Delta_{\text{r}}G = -11.6 \text{ kcal mol}^{-1}$ ), consistent with Scheme 2. However, as expected (*vide supra*),  $\Delta_{\text{r}}G$  for the  $\text{Ar}^{\text{F}}$  analogue of **cis-18** was much more favorable ( $-13.6 \text{ kcal mol}^{-1}$ ), suggesting that the reaction to form **19** is under kinetic control.

Consistent with this hypothesis, when previously isolated **19** was heated at  $60^\circ\text{C}$  in  $\text{C}_6\text{D}_6$  solution for 16 h, quantitative conversion to two new metallacyclic species *cis*- and *trans*- $\text{Ti}(\text{N}_2^{\text{iPr}}\text{N}^{\text{Me}})\{\text{N}\{\text{B}(\text{NAr}'\text{CH})_2\}\text{C}(\text{H})\text{C}(\text{Ar}^{\text{F}})\}$  (**cis**- and **trans-20**, Eq. 4) were formed in a *ca* 3:1 ratio (this ratio was maintained throughout the reaction). In the  $^1\text{H}$  NMR spectrum of **20** the metallacycle methine resonances are observed at 9.29 and 10.32 ppm, respectively, for the major and minor isomers, and a resonance at 22.7 ppm was observed in the  $^{11}\text{B}$  NMR spectrum. On the preparative



scale, a solution of **11** and  $\text{Ar}^{\text{F}}\text{CCH}$  were heated in toluene at 60 °C for 16 h, giving compound **20** as a waxy brown solid in 73% isolated yield after work up.



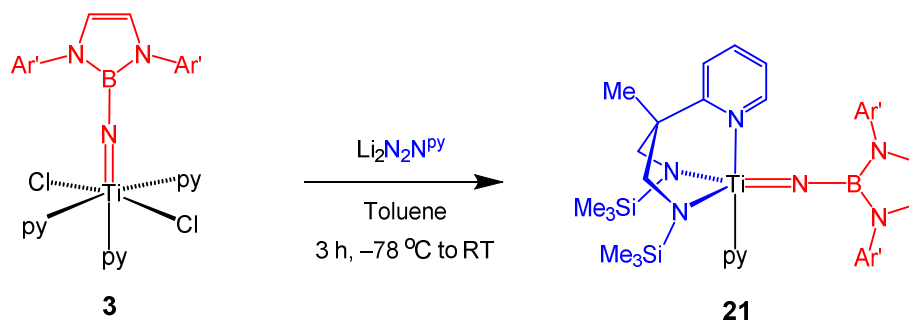
**Equation 4**

The observation of both [2+2] cycloaddition and C–H bond activation being observed for the same imido compound as a function of varying the terminal alkyne (and their interconversion) is relatively uncommon. Bercaw reported that cationic  $[\text{Cp}^*_2\text{Ta}(\text{N}^t\text{Bu})(\text{THF})]^+$  reacts with  $\text{MeCCCH}$  at 25 °C to form a 2:3 mixture of cycloaddition and C–H activation products which were driven to the amide-acetylide  $[\text{Cp}^*_2\text{Ta}\{\text{N}(\text{H})^t\text{Bu}\}(\text{CCMe})]^+$  on heating; reaction with  $\text{PhCCCH}$  gave exclusively  $[\text{Cp}^*_2\text{Ta}\{\text{N}(\text{H})^t\text{Bu}\}(\text{CCPh})]^+$  suggesting that in this case the amide-acetylide isomer is thermodynamically favored over the metallacycle.<sup>29</sup> Bergman and Andersen found that reaction of the isolobal oxo compound  $\text{Cp}^*_2\text{Ti}(\text{O})(\text{py})$  with terminal alkynes gave an equilibrium mixture of oxametallacycle and hydroxide-acetylide products; for the products formed with  $\text{PhCCCH}$ , the two were almost isoenergetic ( $\Delta H = -2.7 \pm 0.4 \text{ kcal mol}^{-1}$  in favor of the metallacycle) and the kinetic and equilibrium effects associated with their interconversion could be determined.<sup>28</sup> In contrast, reaction of  $\text{Cp}^*_2\text{Ti}(\text{NPh})$  with  $\text{RCCH}$  gave only the amide-acetylide  $\text{Cp}^*_2\text{Ti}\{\text{N}(\text{H})\text{Ph}\}(\text{CCR})$  ( $\text{R} = \text{Ph}$  or  $\text{SiMe}_3$ ), whereas  $\text{HCCH}$  exclusively formed the metallacycle product.<sup>16a</sup> Finally, Bergman has proposed (on the basis of kinetic isotope data) that the reaction of  $\text{Cp}^*\text{CpZr}(\text{N}^t\text{Bu})(\text{THF})$  with  $^t\text{BuCCCH}$  to form the amide-acetylide  $\text{Cp}^*\text{CpZr}\{\text{N}(\text{H})^t\text{Bu}\}(\text{CC}^t\text{Bu})$  proceeds *via* a (non-observed) metallacycle intermediate.<sup>30</sup>

We were interested to gain further insight into the mechanistic and energetic aspects of these alkyne C–H addition/elimination reactions of borylimido complexes, and to search for further examples of this type of kinetic *vs* thermodynamic control. Furthermore, the C–H activation reaction of **11** with  $\text{Ar}^{\text{F}}\text{CCH}$  was too fast for convenient kinetic NMR analysis. We therefore turned to a related supporting group, namely the diamide-pyridine ligand  $\text{N}_2\text{N}^{\text{Py}}$  ( $(2\text{-C}_5\text{H}_4\text{N})\text{CMe}(\text{CH}_2\text{NSiMe}_3)_2$ ) which has been found to be extremely useful in synthetic and mechanistic studies (experiment and DFT) of Group 4 organoimido and other metal-ligand multiple bond chemistry.<sup>1d, 16c, 18</sup>

### Synthesis, reactivity and mechanistic studies of $\text{Ti}(\text{N}_2\text{N}^{\text{py}})\{\text{NB}(\text{NAr}'\text{CH})_2\}(\text{py})$ (**21**)

Reaction of  $\text{Ti}\{\text{NB}(\text{NAr}'\text{CH})_2\}\text{Cl}_2(\text{py})_3$  (**3**) and  $\text{Li}_2\text{N}_2\text{N}^{\text{py}}$  in toluene at  $-78^\circ\text{C}$ , followed by extraction into pentane produced analytically pure  $\text{Ti}(\text{N}_2\text{N}^{\text{py}})\{\text{NB}(\text{NAr}'\text{CH})_2\}(\text{py})$  (**21**, Eq. 5) as an orange solid in 83% yield. The  $^1\text{H}$  and  $^{13}\text{C}$  NMR spectra of **21** indicate  $C_s$  symmetry as indicated. The  $^{11}\text{B}$  chemical shift of the borylimido ligand is 14.5 ppm, which is in good agreement with the DFT calculated (see later studies) value of 15.7 ppm and the values found for **9** – **11**.



Equation 5

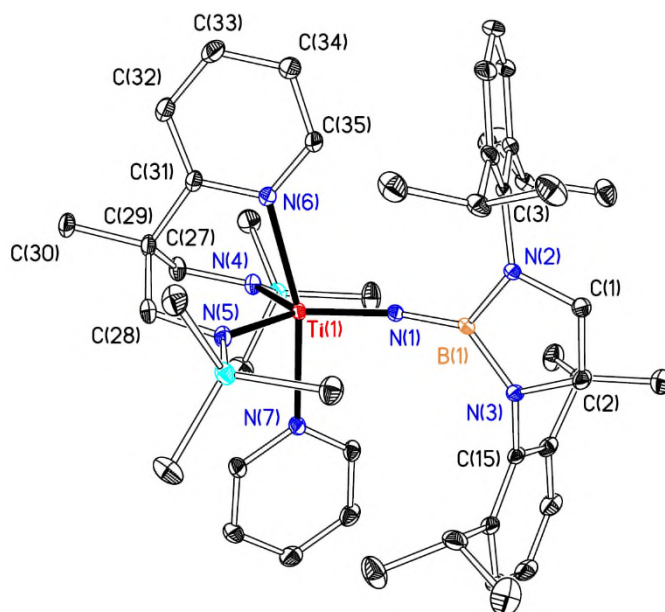
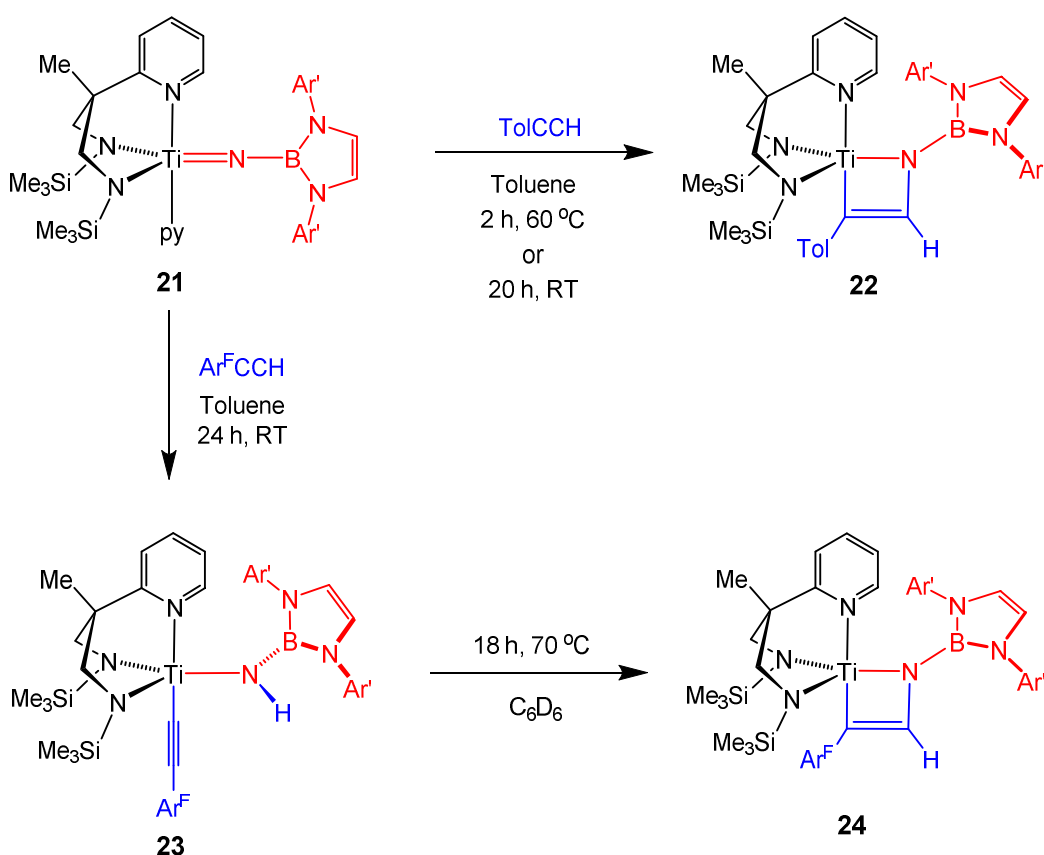


**Figure 6.** Displacement ellipsoid plot (20% probability) of  $\text{Ti}(\text{N}_2\text{N}^{\text{py}})\{\text{NB}(\text{NAr}'\text{CH})_2\}(\text{py})$  (**21**). H atoms are omitted for clarity. Selected bond distances (Å) and angles ( $^\circ$ ):  $\text{Ti}(1)\text{--N}(1)$  1.7727(6) [1.7604(7)],  $\text{Ti}(1)\text{--N}(4)$  1.9860(7) [1.9757(7)],  $\text{Ti}(1)\text{--N}(5)$  1.9648(7) [1.9734(7)],  $\text{Ti}(1)\text{--N}(6)$  2.2105(7) [2.2002(7)],  $\text{Ti}(1)\text{--N}(7)$  2.2450(7) [2.2576(7)],  $\text{N}(1)\text{--B}(1)$  1.4149(11) [1.4185(11)],  $\text{Ti}(1)\text{--N}(1)\text{--B}(1)$  159.95(6) [167.32(6)].  $\tau = 0.64$  [0.62]. Values in brackets are for the second crystallographically independent molecule.

Diffraction-quality crystals of **21** were grown from pentane. The solid state structure is shown in Figure 6 along with selected bond lengths and angles. Molecules of **21** have the expected distorted

trigonal bipyramidal coordination geometry in the solid state. The average Ti–N<sub>imide</sub> bond lengths of 1.767(1) Å (for two crystallographically independent molecules) is comparable to that of the N<sub>2</sub><sup>iPr</sup>N<sup>Me</sup>-supported **11** (1.760(2) Å) and considerably longer than in the *tert*-butylimide Ti(N<sub>2</sub>N<sup>py</sup>)(N<sup>tBu</sup>)(py) (1.724(2) Å)<sup>18b</sup> as expected on electronic<sup>10</sup> and steric grounds.

On the NMR tube scale in C<sub>6</sub>D<sub>6</sub>, the reaction of **21** with TolCCH proceeded more slowly than the same reaction with **11**. However, heating at 60 °C for 2 h resulted in quantitative conversion to the azatitanacyclobutene complex Ti(N<sub>2</sub>N<sup>py</sup>){N{B(NAr'CH)<sub>2</sub>}C(H)C(Tol)} (**22**). Similarly, the NMR tube scale reaction of Ar<sup>F</sup>CCH with **21** proceeded more slowly than that with **11**, but after 16 h at room temperature, quantitative conversion to the borylamide-acetylide complex, Ti(N<sub>2</sub>N<sup>py</sup>){NHB(NAr'CH)<sub>2</sub>}(CCAr<sup>F</sup>) (**23**), had taken place. The compounds were obtained in analytically pure form after scale-up in toluene (Scheme 3). Table 2 summarizes the Δ<sub>r</sub>G values for the formation of **22**, **23** and their isomers and selected isotopomers. As was found for **9** – **11**, no reaction was found between **21** and other alkynes, including PhCCMe and MeCCMe, in agreement with the endergonic Δ<sub>r</sub>G values by DFT.



**Scheme 3.** Reactions of Ti(N<sub>2</sub>N<sup>py</sup>){NB(NAr'CH)<sub>2</sub>}(py) (**21**) with ArCCH (Ar = Tol or Ar<sup>F</sup>).

The <sup>1</sup>H NMR spectrum of **22** indicates a single isomer of an azatitanacyclobutene complex with anti-Markovnikov type regiochemistry. The metallacycle methine is observed at 9.56 ppm. The <sup>11</sup>B

chemical shift of 25.5 ppm is in good agreement with the DFT calculated value of 26.9 ppm. The  $^1\text{H}$  NMR spectrum of **23** is comparable to that of its analogue **19**. A broad NH singlet is observed at 6.08 ppm and the two acetylide carbons  $\text{TiCCAr}^{\text{F}}$  are observed at 161.1 and 87.6 ppm in the  $^{13}\text{C}$  NMR spectrum. The  $^{11}\text{B}$  shift is 23.0 ppm, in good agreement with the DFT value of 24.9 ppm.  $\nu(\text{C}\equiv\text{C})$  is observed at  $2096\text{ cm}^{-1}$  (DFT:  $2100\text{ cm}^{-1}$ ) in the IR spectrum, which is very similar to that for **19** ( $2094\text{ cm}^{-1}$ ).

As for the reactions of **11** with  $\text{ArCCH}$ , the  $\Delta_{\text{r}}G$  DFT results in Table 2 show that although the formation of **23** is exergonic, its metallacycle isomer (the analogue of **22**) is thermodynamically more stable. Accordingly, heating of **23** at  $70\text{ }^{\circ}\text{C}$  for 18 h in  $\text{C}_6\text{D}_6$  resulted in quantitative conversion to the azatitanacyclobutene complex  $\text{Ti}(\text{N}_2\text{N}^{\text{py}})\{\text{N}\{\text{B}(\text{NAr}'\text{CH})_2\}\text{C}(\text{H})\text{C}(\text{Ar}^{\text{F}})\}$  (**24**, Scheme 3). On the preparative scale, **24** was isolated as a dark brown solid in 64% yield after heating **21** and  $\text{Ar}^{\text{F}}\text{CCH}$  in toluene at  $60\text{ }^{\circ}\text{C}$  for 40 hs. The  $^1\text{H}$  and  $^{13}\text{C}$  NMR spectra of **24** are consistent with a single isomer of anti-Markovnikov type regiochemistry.

Diffraction-quality crystals of **22** and **23** were grown from hexane. The solid state structures are shown in Fig. 7 along with selected bond distances and angles. The azatitanacyclobutene complex **22** has an analogous structure to those described above, having a distorted pentacoordinate geometry ( $\tau = 0.50$ ) in which the diamide-pyridine ligand is facially coordinating. The solid state structure confirms its AM type regiochemistry and that the N-boryl group is oriented *cis* to the pyridyl group. The borylamide-acetylide complex **23** also has a distorted pentacoordinate geometry ( $\tau = 0.63$ ), with the diamide-pyridine ligand again being *fac*-coordinating. The borylamide ligand occupies an equatorial site *cis* to the pyridyl group, and the acetylide ligand is *trans* to pyridyl. The Ti–C bond distance to the acetylide ligand is  $2.1552(10)\text{ \AA}$ , and the  $\text{C}\equiv\text{C}$  bond distance of  $1.2143(15)\text{ \AA}$  is consistent with a triple bond.

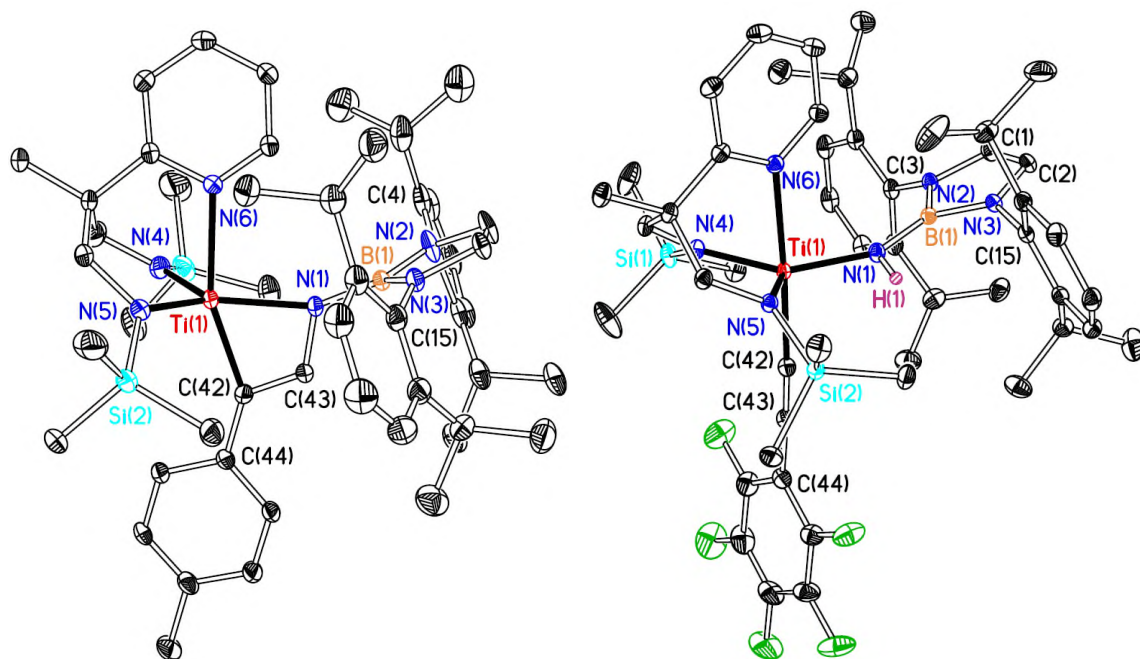
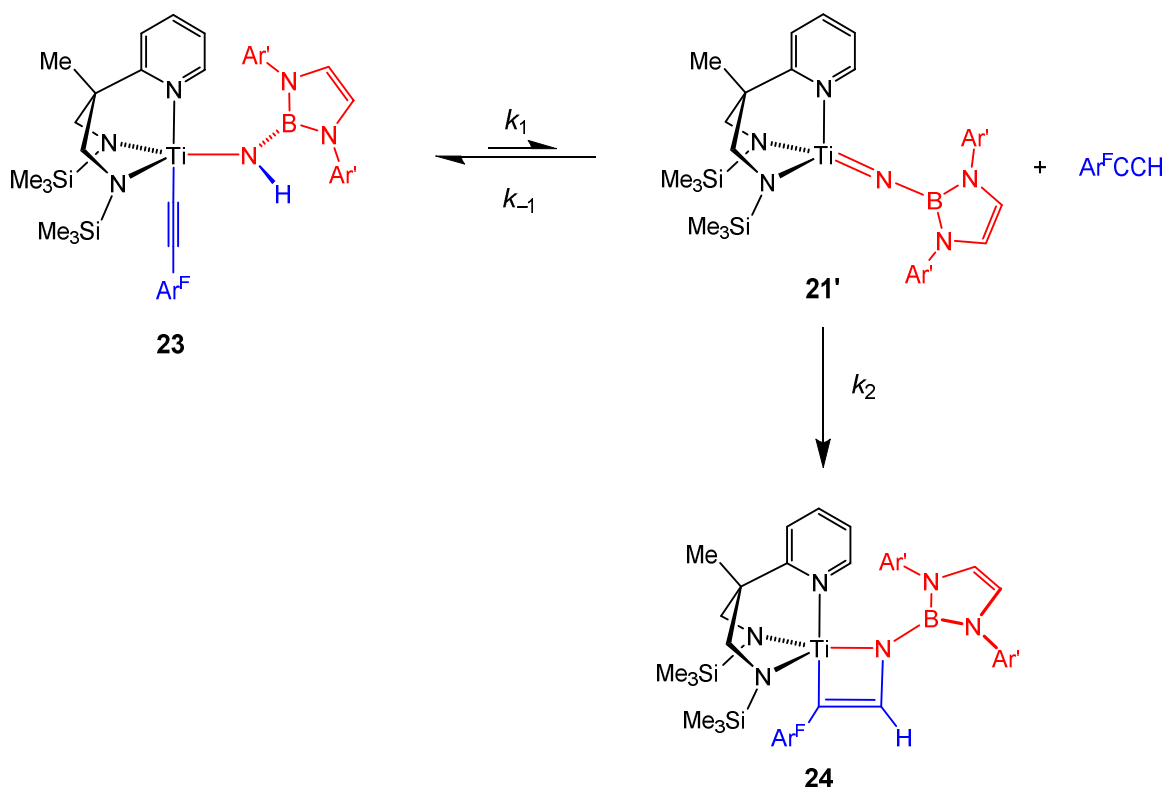


**Figure 7.** Displacement ellipsoid plot (25% probability) of  $\text{Ti}(\text{N}_2\text{N}^{\text{py}})\{\text{N}\{\text{B}(\text{NAr}'\text{CH})_2\}\text{C}(\text{H})\text{C}(\text{Tol})\}$  (**22**, left) and  $\text{Ti}(\text{N}_2\text{N}^{\text{py}})\{\text{NHB}(\text{NAr}'\text{CH})_2\}(\text{CCAr}^{\text{F}})$  (**23**, right). H atoms are omitted for clarity except for H(1) of **23** which is drawn as a sphere of arbitrary radius. Selected bond distances (Å) and angles (°) for **22**: Ti(1)–N(1) 2.062(2), Ti(1)–N(4) 1.911(3), Ti(1)–N(5) 1.907(3), Ti(1)–N(6) 2.283(2), Ti(1)–C(42) 2.053(3), N(1)–B(1) 1.429(3), N(1)–C(43) 1.380(3), C(42)–C(43) 1.320(4), N(1)–Ti(1)–C(42) 69.58(9), Ti(1)–N(1)–B(1) 152.40(18), Ti(1)–C(42)–C(43) 85.61(17), N(1)–C(43)–C(42) 120.8(2) ( $\tau = 0.50$ ); for **23**: Ti(1)–N(1) 1.9591(8), Ti(1)–N(4) 1.9236(8), Ti(1)–N(5) 1.8841(8), Ti(1)–N(6) 2.2774(8), Ti(1)–C(42) 2.1552(10), N(1)–B(1) 1.4269(13), N(1)–H(1) 0.908(16), C(42)–C(43) 1.2143(15), Ti(1)–N(1)–B(1) 155.66(7), Ti(1)–C(42)–C(43) 177.30(8) ( $\tau = 0.63$ ).

The slower rate of reaction between  $\text{Ti}(\text{N}_2\text{N}^{\text{py}})\{\text{NB}(\text{NAr}'\text{CH})_2\}(\text{py})$  (**21**) and  $\text{Ar}^{\text{F}}\text{CCH}$  to give the borylamide-acetylide **23** allowed measurement of the initial rate of this reaction and for the corresponding reaction with  $\text{Ar}^{\text{F}}\text{CCD}$  forming the isotopomer  $\text{Ti}(\text{N}_2\text{N}^{\text{py}})\{\text{NDB}(\text{NAr}'\text{CH})_2\}(\text{CCAr}^{\text{F}})$  (**23-d1**) as summarised in Fig. S7 of the SI. For the reaction with  $\text{Ar}^{\text{F}}\text{CCH}$  the initial rate of the reaction was  $20.1(1) \times 10^{-6} \text{ mol dm}^{-3} \text{ s}^{-1}$  (av. of two experiments). The corresponding reaction with  $\text{Ar}^{\text{F}}\text{CCD}$  gave the initial rate of the reaction as  $3.9(1) \times 10^{-6} \text{ mol dm}^{-3} \text{ s}^{-1}$  (again performed in duplicate). The computed kinetic isotope effect (KIE) for this reaction is therefore 5.1(1), consistent with C–H bond activation being the rate-determining step. Previous studies of the reactions of organoimido and hydrazido analogues of **21** and its counterparts have shown that they proceed *via* facile pyridine loss<sup>8a, 16c, d, 18e</sup> to form four-coordinate complexes of the type  $\text{Ti}(\text{N}_2\text{N}^{\text{py}})(\text{NR})$ , which have been isolated in certain cases.<sup>18b</sup> DFT calculations for **21** showed that  $\Delta_r G$  for formation of the base-free  $\text{Ti}(\text{N}_2\text{N}^{\text{py}})\{\text{NB}(\text{NAr}'\text{CH})_2\}$  (**21'**) and pyridine was only 10.7 kcal mol<sup>−1</sup> at room temperature

( $\Delta_r H = 19.1 \text{ kcal mol}^{-1}$ ), giving an upper limit<sup>31</sup> of *ca.*  $1.8 \times 10^{-3} \text{ mol dm}^{-3} \text{ s}^{-1}$  for the rate of formation of the reactive intermediate **21'**, consistent with C–H bond activation being rate-determining according to experiment.

The KIE of 5.1(1) is consistent with values reported for a number of other C–H bond activation and formation processes at Group 4 metal centers.<sup>4b, 28, 30, 32</sup> The magnitudes of such isotope effects and their origins have been discussed in these previous papers and reviews.<sup>11, 33</sup> The KIE for the reaction of **21** is indicative of a process having a transition state in which the transfer of H is relatively linear.<sup>34</sup> We discuss the geometry of the DFT computed transition state later on in this paper.



**Scheme 4.** Mechanism for the conversion of  $\text{Ti}(\text{N}_2\text{N}^{\text{Py}})\{\text{NHB}(\text{NAr}'\text{CH})_2\}(\text{CCAr}^{\text{F}})$  (**23**) to  $\text{Ti}(\text{N}_2\text{N}^{\text{Py}})\{\text{N}\{\text{B}(\text{NAr}'\text{CH})_2\}\text{C}(\text{H})\text{C}(\text{Ar}^{\text{F}})\}$  (**24**).

The conversion of the borylamide-acetylides **23** and **23-d<sub>1</sub>** to the corresponding azatitanacyclobutene complexes **24** and **24-d<sub>1</sub>** was analysed further by  $^1\text{H}$  NMR spectroscopy at 343 K. The decay of **23** and **23-d<sub>1</sub>** follows first order kinetics as judged by semi-logarithmic plots of  $-\ln([\mathbf{23}]/[\mathbf{23}]_0)$  and  $-\ln([\mathbf{23-d_1}]/[\mathbf{23-d_1}]_0)$  vs. time (Fig. S8 of the SI). The observed rate constants (each measured in duplicate) are  $k_{\text{obs}(\text{H})} = 4.1(1) \times 10^{-5} \text{ s}^{-1}$  and  $k_{\text{obs}(\text{D})} = 3.1(1) \times 10^{-5} \text{ s}^{-1}$  for **23** and **23-d<sub>1</sub>**, respectively, giving an overall KIE of 1.3(1). The associated  $\Delta G_{343}^\ddagger$  values for these two reactions are 27.0 and 27.2  $\text{kcal mol}^{-1}$  ( $\Delta\Delta G_{343}^\ddagger = 0.2 \text{ kcal mol}^{-1}$ ), respectively.

Scheme 4 shows the proposed mechanism for rearrangement of **23** to **24** which proceeds via  $\text{Ar}^{\text{F}}\text{CCH}$  elimination to form transient **21'** (not observed), followed by [2+2] cycloaddition. Evidence for alkyne dissociation comes from a crossover experiment in which thermolysis of **23** in the presence of 1 equiv.  $\text{Ti}(\text{N}_2^{\text{iPr}}\text{N}^{\text{Me}})\{\text{NB}(\text{NAr}'\text{CH})_2\}(\text{py})$  (**11**, shown above to react quickly with  $\text{Ar}^{\text{F}}\text{CCH}$ ) formed a mixture of the two metallacycles,  $\text{Ti}(\text{N}_2^{\text{iPr}}\text{N}^{\text{Me}})\{\text{N}\{\text{B}(\text{NAr}'\text{CH})_2\}\text{C}(\text{H})\text{C}(\text{Ar}^{\text{F}})\}$  (**20**) and **24** in a 5:1 molar ratio. The rate expression for Scheme 4 is shown in Eq. 6. The approximation  $k_{-1} \gg k_2$  applies because the reaction of  $\text{Ar}^{\text{F}}\text{CCH}$  with the borylimide **21** (precursor to **21'**) to form **23** is fast at room temperature, whereas formation of **24** requires elevated temperatures. Thus, the observed 1<sup>st</sup> order rate constants ( $k_{\text{obs}}$ ) are a combination of the equilibrium constant ( $k_1/k_{-1}$ ) between **23** and dissociated **21'** +  $\text{Ar}^{\text{F}}\text{CCH}$ , and the rate constant ( $k_2$ ) for cycloaddition. The latter is effectively isotope-insensitive (no C–H bond cleavage; cf. DFT studies below). Therefore the value of the overall KIE for **23**  $\rightarrow$  **24** ( $k_{\text{obs}(\text{H})} / k_{\text{obs}(\text{D})}$ ) is in fact the equilibrium isotope effect (EIE) between **23** and **21'** +  $\text{Ar}^{\text{F}}\text{CCH}$ . In support of this, we found that the difference ( $\Delta\Delta G_{343}^\ddagger$ ) of *ca.* 0.20 kcal mol<sup>-1</sup> between the Gibbs free energies of dissociation for **23** and **23-d1** obtained from the kinetic analyses agrees well with the difference between the computed values for the reaction of **21** with  $\text{Ar}^{\text{F}}\text{CCH}$  or  $\text{Ar}^{\text{F}}\text{CCD}$  ( $\Delta\Delta_r G_{343} = 0.17$  kcal mol<sup>-1</sup>, Table 2). This  $\Delta\Delta_r G$  (and therefore EIE) arises from deuterium preferring to reside in the higher energy bond (N–H), since the difference in zero point energy (ZPE) between an E–H and E–D bond increases with vibrational frequency.<sup>34a, 35</sup> A very similar EIE of 1.28 was reported by Bergman and Andersen for the conversion of the hydroxide-acetylide  $\text{Cp}^*_2\text{Ti}(\text{OH})(\text{CCPh})$  to the metallacycle  $\text{Cp}^*_2\text{Ti}\{\text{OC}(\text{Ph})\text{C}(\text{H})\}$  via  $\text{Cp}^*_2\text{Ti}(\text{O})$ .<sup>28</sup>

$$\frac{d[\mathbf{24}]}{dt} = k_2[\mathbf{21}'][\text{Ar}^{\text{F}}\text{CCH}] = \frac{k_1 k_2 [\mathbf{23}]}{k_{-1} + k_2}$$

$$\text{Since } k_{-1} \gg k_2: \frac{d[\mathbf{24}]}{dt} = \frac{k_1 k_2 [\mathbf{23}]}{k_{-1}}$$

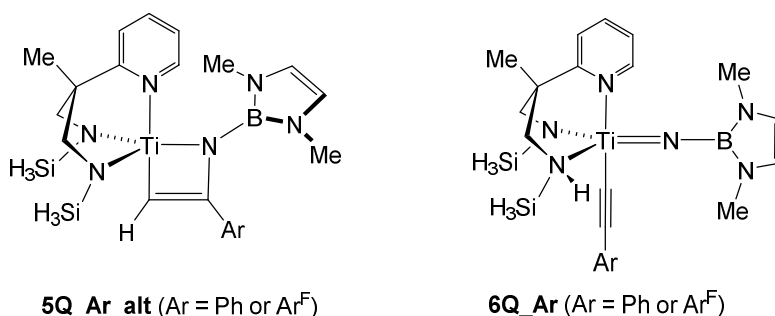
### Equation 6

#### Further DFT studies: [2+2] cycloaddition vs. C–H bond activation

Table 2 gives DFT computed Gibbs free energies of reaction ( $\Delta_r G$ ) of certain alkynes and their isotopomers with  $\text{Ti}(\text{N}_2^{\text{R}}\text{N}^{\text{Me}})\{\text{NB}(\text{NAr}'\text{CH})_2\}(\text{py})$  (**9** – **11**) and  $\text{Ti}(\text{N}_2\text{N}^{\text{Py}})\{\text{NB}(\text{NAr}'\text{CH})_2\}(\text{py})$  (**21**). These results are for the full experimental systems, including corrections for dispersion and solvent effects. Because of the size and number of the systems involved, it was not feasible to conduct a mechanistic DFT study of the full systems. A sterically pruned version of **21**,

$\text{Ti}(\text{N}_2^{\text{SiH}_3\text{N}^{\text{py}}})\{\text{NB}(\text{NMeCH})_2\}(\text{py})$  (**1Q**), in which the  $\text{SiMe}_3$  groups are replaced by  $\text{SiH}_3$ , and the  $\text{B}(\text{NAr}^{\text{F}}\text{CH})_2$  groups by  $\text{B}(\text{NMeCH})_2$  was therefore studied by DFT to probe the underlying electronic factors operating in this system. These results complement the other DFT data in Table 2 and the experimental results. Fig. 8 summarises the main reactions of **1Q** with  $\text{PhCCH}$  (as a model for  $\text{TolCCH}$ ) and  $\text{Ar}^{\text{F}}\text{CCH}$ . Further details of the methodology and the geometries of the systems are given in the Supporting Information.

Fig.8 focuses on the underlying the kinetic and thermodynamic preferences of  $\text{ArCCH}$  ( $\text{Ar} = \text{Ph}$  or  $\text{Ar}^{\text{F}}$ ) for C–H activation (forming **3Q\_Ar**) or AM type [2+2] cycloaddition (forming **5Q\_Ar**). The Markovnikov type isomers  $\text{Ti}(\text{N}_2^{\text{SiH}_3\text{N}^{\text{py}}})\{\text{N}\{\text{B}(\text{NMeCH})_2\}\text{C}(\text{Ar})\text{C}(\text{H})\}$  (**5Q\_Ar\_alt**) were found to be 3.5 or 7.4  $\text{kcal mol}^{-1}$  less stable for  $\text{Ar} = \text{Ph}$  or  $\text{Ar}^{\text{F}}$ , respectively. In principle, C–H activation could take place the  $\text{Ti}-\text{N}_{\text{amide}}$  bonds to form imido-acetylide compounds **6Q\_Ar**. However, these lie at  $\Delta G = 13.6$  and  $17.0 \text{ kcal mol}^{-1}$  above the starting **1Q** and  $\text{ArCCH}$ , and the transition states (TSs) leading to them are at  $25.9$  and  $26.4 \text{ kcal mol}^{-1}$ , are clearly unfavorable.



The trends in relative stabilities of the C–H activation (**3Q\_Ar**) and cycloaddition (**5Q\_Ar**) products are consistent with the experimental data. **3Q\_Ar<sup>F</sup>** is clearly the kinetic product for  $\text{Ar}^{\text{F}}\text{CCH}$ , and the transition states (**TS1\_Ar<sup>F</sup>** and **TS2\_Ar<sup>F</sup>**) for the isomerization **3Q\_Ar<sup>F</sup>**  $\rightarrow$  **2Q**  $\rightarrow$  **3Q\_Ar<sup>F</sup>** is energetically accessible, with the computed  $\Delta G_{343}^\ddagger$  value of  $23.8 \text{ kcal mol}^{-1}$  at 343 K (*cf.* Fig. S9 of the SI for the  $G_{\text{rel}}$  values at 343 K) agreeing reasonably well with the experimental value of  $27.0 \text{ kcal mol}^{-1}$  for the full experimental system (i.e. **23**  $\rightarrow$  **24**). The electron-withdrawing  $\text{Ar}^{\text{F}}$  ring in **5Q\_Ar<sup>F</sup>** stabilizes this compound relative to **5Q\_Ph** significantly ( $\Delta G = 5.5 \text{ kcal mol}^{-1}$ ), as expected from previous experimental data for related metallacycles.<sup>16d, 18e, 22</sup> Likewise **3Q\_Ar<sup>F</sup>** is more stable than **3Q\_Ph**, with the latter being almost endergonic in this small model system. For the corresponding real systems listed in Table 2, none of the C–H bond activation products with  $\text{TolCCH}$  were predicted to be stable. Although the C–H bond strength in  $\text{Ar}^{\text{F}}\text{CCH}$  is stronger than that in  $\text{PhCCH}$  or  $\text{TolCCH}$ , the C–H bond activation products are more stable for the former because  $\text{M}-\text{CCAr}$  bond enthalpies also increase in the same way but at a slightly faster rate,<sup>36</sup> reflecting a more general situation in transition metal thermochemistry.<sup>37</sup>



The transition state for C–H bond cleavage (**TS1\_Ar**) has a fairly linear C–H–Ti–N<sub>imide</sub> (e.g. 156.5 ° in **TS1\_Ar<sup>F</sup>**) arrangement as expected with C–H and N<sub>imide</sub>–H distances of 1.298 and 1.439 Å (for **TS1\_Ar<sup>F</sup>**). The TS for Ar<sup>F</sup>CCH (**TS1\_Ar<sup>F</sup>**) is 1.1 kcal mol<sup>–1</sup> more stable than for PhCCH (**TS1\_Ph**) and occurs slightly earlier along the reaction coordinate as judged by the longer C–H, and shorter N<sub>imide</sub>–H, distances of 1.315 and 1.419 Å, respectively, in **TS1\_Ph**. At 343 K (*cf.* Fig. S9 in the SI) the  $\Delta G_{343}^\ddagger$  values for the formation of **3Q\_Ar<sup>F</sup>** and **3Q\_Ar<sup>F</sup>-d<sub>1</sub>** from **1Q** and either Ar<sup>F</sup>CCH or Ar<sup>F</sup>CCD are 20.4 and 21.3 kcal mol<sup>–1</sup>, resulting in a computed KIE of 3.4 (*cf.* 5.1 based on the experimental system **21** + Ar<sup>F</sup>CCH or Ar<sup>F</sup>CCD → **23** or **23-d<sub>1</sub>**). The computed EIE between **3Q\_Ar<sup>F</sup>** or **3Q\_Ar<sup>F</sup>-d<sub>1</sub>** and **2Q** is 1.23 at 343 K which compares very well with the experimental value of 1.3(1).

As expected, the calculations predict no significant KIE for [2+2] cycloaddition (transition state **TS2\_Ar** ( $\Delta G_{343}^\ddagger = 20.7$  for both Ar<sup>F</sup>CCH and Ar<sup>F</sup>CCD), Fig. S9). In the case of the reaction with PhCCH, this TS (i.e. **TS2\_Ph**) is preceded by a  $\pi$ -adduct **4Q\_Ph** which is not stable for the more electron deficient Ar<sup>F</sup>CCH (dissociates to Ar<sup>F</sup>CCH and **2Q** on attempted geometry optimization). Furthermore, both of the cycloaddition transition states **TS2\_Ar** feature significant  $\eta^2$ -alkyne C $\equiv$ C→Ti  $\pi$ -donation which is more developed for **TS2\_Ph** than for **TS2\_Ar<sup>F</sup>** as judged by shorter Ti⋯C<sub>alkyne</sub> distances in the former (2.244 and 2.331 vs. 2.291 and 2.353 Å). These features may help explain why **TS2\_Ph** is slightly more stable ( $\Delta\Delta G^\ddagger = 0.2$  kcal mol<sup>–1</sup>) than **TS2\_Ar<sup>F</sup>**, even though, for the cycloaddition products **5Q\_Ph** and **5Q\_Ar<sup>F</sup>** themselves, the phenyl substituted system is significantly less stable ( $\Delta\Delta_r G = 5.5$  kcal mol<sup>–1</sup>) for the reasons described earlier. Recall that, experimentally, the competition reaction between Ti(N<sub>2</sub><sup>SiMe<sub>3</sub></sup>N<sup>Me</sup>){NB(NAr'CH)<sub>2</sub>}(py) (**9**) and an excess of TolCCH and of Ar<sup>F</sup>CCH gave a *ca.* 2:1 molar ratio mixture of Ti(N<sub>2</sub><sup>SiMe<sub>3</sub></sup>N<sup>Me</sup>){N{B(NAr'CH)<sub>2</sub>}C(H)C(Tol)} (**12**) and Ti(N<sub>2</sub><sup>SiMe<sub>3</sub></sup>N<sup>Me</sup>){N{B(NAr'CH)<sub>2</sub>}C(H)C(Ar<sup>F</sup>)} (**13**), apparently consistent with the TS for [2+2] cycloaddition with TolCCH being slightly more accessible (and certainly competitive), despite the very different computed  $\Delta\Delta_r G$  (5.6 kcal mol<sup>–1</sup>, Table 2) for forming **12** and **13** from **9**.

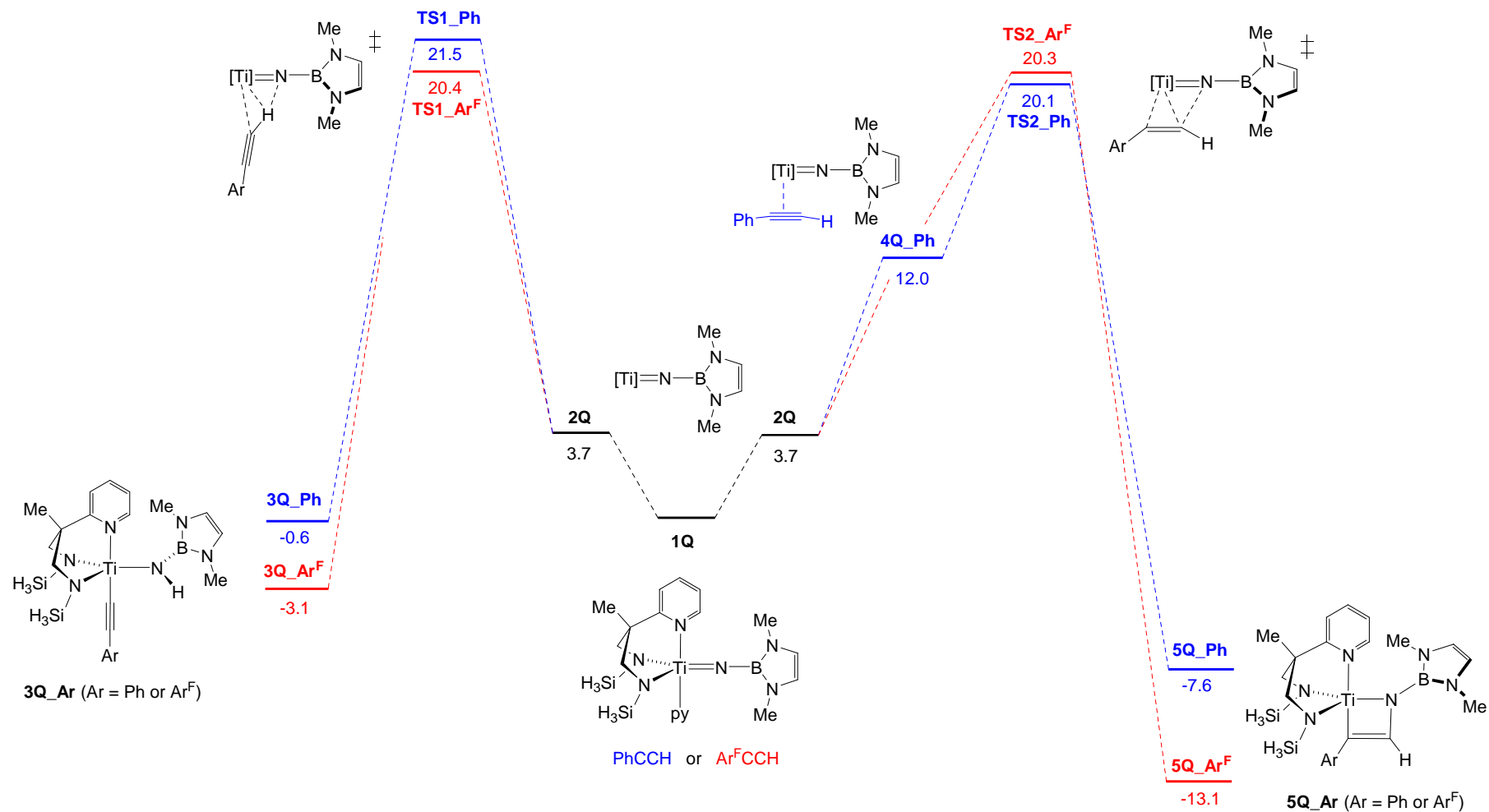
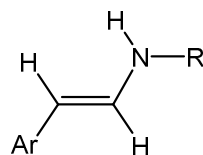
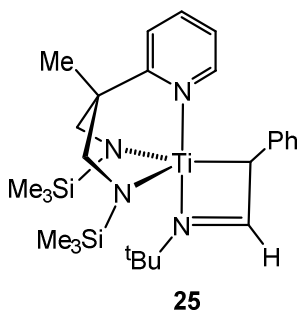


**Figure 8.** Relative Gibbs free energies ( $G_{\text{rel}}$ , kcal mol<sup>-1</sup>) at 298 K for the DFT computed reactions of  $\text{Ti}(\text{N}_2^{\text{SiH}_3}\text{N}^{\text{py}})\{\text{NB}(\text{NMeCH})_2\}(\text{py})$  (**1Q**) with  $\text{Ar}^{\text{F}}\text{CCH}$  and  $\text{PhCCH}$ .

Although the small model systems in Fig. 8 and Fig. S9 of the SI successfully account for and rationalise many of the experimental features of the real systems, the relative Gibbs free energies of activation for **TS2\_Ar** is probably somewhat underestimated since in at least the reactions of  $\text{Ti}(\text{N}_2^{\text{iPr}}\text{N}^{\text{Me}})\{\text{NB}(\text{NAr}'\text{CH})_2\}(\text{py})$  (**11**) and  $\text{Ti}(\text{N}_2\text{N}^{\text{py}})\{\text{NB}(\text{NAr}'\text{CH})_2\}(\text{py})$  (**21**) with  $\text{Ar}^{\text{F}}\text{CCH}$ , the C–H activation products (**19** and **23**, respectively), are kinetically favored. Gade *et al.* have noted a similar problem previously in modelling large experimental systems with smaller, computationally tractable models for alkyne C–H activation *vs.* [2+2] cycloaddition.<sup>38</sup> Inspection of the DFT structures of **TS1\_Ar** and **TS2\_Ar** (see the SI and depictions in Figs. 8 and S9) show clearly that, in a real experimental system with much more significant steric bulk, the more hindered transition state for cycloaddition (**2Q\_Ar**) in which the alkyne approaches the Ti–N<sub>imide</sub> bond side-on would be expected to be destabilised somewhat more than **TS1\_Ar** in which the alkyne approaches rather more end-on in a  $\sigma$ -fashion

### Attempted hydroborylamination of alkynes

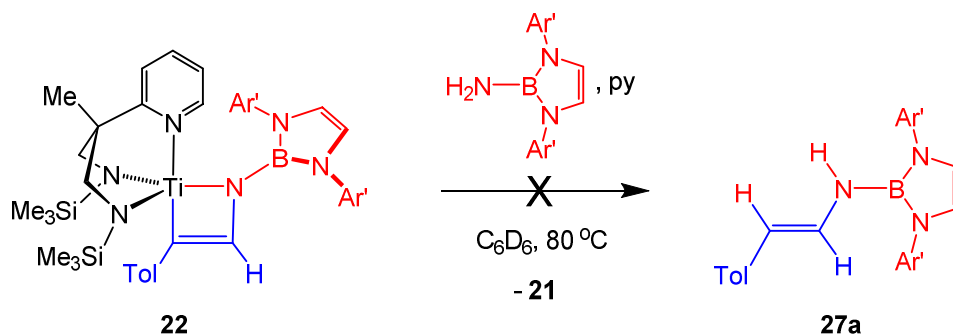
The hydroamination and hydrohydrazination of alkynes by Group 4 imido and hydrazido catalysts has remained a focus of study in this field<sup>1h-j, 17a-e</sup> since Bergman's initial reports<sup>1b, 17f</sup> over 20 years ago. As revealed by elegant mechanistic and computational<sup>39</sup> studies, azatitanacyclobutene-type compounds are the crucial intermediates in this catalysis, undergoing protolysis with added external primary amine to regenerate the reactive imide and the product enamine or its imine tautomer. In particular, in Gade *et al.* have shown that the diamide-pyridine supported organoimido compound  $\text{Ti}(\text{N}_2\text{N}^{\text{py}})(\text{N}^{\text{tBu}})(\text{py})$  and various homologues act as catalysts for the anti-Markovnikov hydroamination of terminal alkynes.<sup>16b, c</sup> Explicitly it was shown that the key metallacycle intermediate *trans*- $\text{Ti}(\text{N}_2\text{N}^{\text{py}})\{\text{N}^{\text{tBu}}\text{C}(\text{H})\text{C}(\text{Ph})\}$  (**25**) reacted with  $^{\text{tBu}}\text{NH}_2$  in the presence of pyridine to regenerate  $\text{Ti}(\text{N}_2\text{N}^{\text{py}})(\text{N}^{\text{tBu}})(\text{py})$  and the enamine  $\text{PhC}(\text{H})=\text{C}(\text{H})\text{N}(\text{H})^{\text{tBu}}$  (**26**).<sup>16b</sup>



Ar = Ph, R =  $^{\text{tBu}}$  (**26**). Ar = Tol,  
R = B(NAr'CH)<sub>2</sub> (**27a**),  $^{\text{tBu}}$  (**27b**), Xyl (**27c**)

Given the successful formation of a number of azatitanacyclobutenes through the reactions of **9**, **10**, **11** and **21** with TolCCH and  $\text{Ar}^{\text{F}}\text{CCH}$ , we also explored the potential of borylamines in hydroamination chemistry (i.e. hydroborylamination) since this has not previously been reported.

Disappointingly, the attempted reactions of the metallacycles **12**, **14**, **18** and **22** with **25** with the borylamine  $\text{H}_2\text{NB}(\text{NAr}'\text{CH})_2$ <sup>11</sup> (with or without 1 equiv. py to regenerate the starting borylimide) were all unsuccessful, as illustrated by Eq. 7 for **22**. On the NMR tube scale at room temperature, no reaction was observed. Upon heating up to 90 °C this led to eventual decomposition of the metallacyclic compound, with no identifiable products.



**Equation 7**

DFT studies suggest that this is a kinetic limitation, probably due to the large bulk of the borylimide group. The computed  $\Delta_r G$  for the formation of the target borylenamine **27a** (Eq. 7) from **22** and  $\text{H}_2\text{NB}(\text{NAr}'\text{CH})_2$  was  $-12.5\text{ kcal mol}^{-1}$ , more exergonic in fact than for the reaction of **25** and  $^t\text{BuNH}_2$  to give  $\text{PhC(H)=C(H)N(H)}^t\text{Bu}$  (**26**) and the corresponding imide ( $\Delta_r G = -4.7$ ). In addition, calculations on the AM hydroamination reactions of selected amines  $\text{RNH}_2$  ( $\text{R} = \text{B}(\text{NAr}'\text{CH})_2$ ,  $^t\text{Bu}$  or Xyl) with  $\text{TolC(H)=C(H)N(H)R}$  found very comparable free energies of reaction:  $\Delta_r G = -27.7$  (**27a**),  $-26.8$  (**27b**), and  $23.0$  (**27c**)  $\text{kcal mol}^{-1}$ .

## Conclusions

Use of the recently reported borylimide  $\text{Ti}\{\text{NB}(\text{NAr}'\text{CH})_2\}\text{Cl}_2(\text{py})_3$  (**3**) with  $\text{Li}_2\text{N}_2^{\text{RMe}}$  and  $\text{Li}_2\text{N}_2^{\text{Npy}}$  has provided access to the first titanium borylimides (**9** – **11** and **21**) supported by these activating,  $\pi$ -donor ligand sets. As found previously for their organoimido counterparts, these do not form [2+2] cycloaddition products with internal alkynes (indicated by DFT calculations to be endergonic). Of the homologous compounds  $\text{Ti}(\text{N}_2^{\text{RMe}})\{\text{NB}(\text{NAr}'\text{CH})_2\}(\text{py})$  ( $\text{R} = \text{SiMe}_3$  (**9**)  $\text{Ar}^{\text{F}}$  (**10**) or  $^i\text{Pr}$  (**11**)), only **11**, having the most strongly donating  $\text{N}_2^{\text{RMe}}$  ligand and longest Ti– $\text{N}_{\text{imide}}$  bond, undergoes C–H bond activation, but only with  $\text{Ar}^{\text{F}}\text{CCH}$  because of the stronger Ti–C bond formed in this case.  $\text{Ti}(\text{N}_2^{\text{Npy}})\{\text{NB}(\text{NAr}'\text{CH})_2\}(\text{py})$  (**21**) also forms an acetylide product with  $\text{Ar}^{\text{F}}\text{CCH}$  in the first instance. All of the azametallacycle products are of the anti-Markovnikov type as expected based on previous work, and confirmed here as being electronically preferred by DFT calculations on sterically pruned systems. The azametallacycle products formed from  $\text{ArCCH}$  and **9**, **11** and **21** are all more stable for  $\text{Ar} = \text{Ar}^{\text{F}}$ ; in the case of the cycloaddition products formed from **10**, however,

intramolecular  $\pi$ -interactions lead to  $\text{Ti}(\text{N}_2^{\text{ArF}}\text{N}^{\text{Me}})\{\text{N}\{\text{B}(\text{NAr}'\text{CH})_2\}\text{C}(\text{H})\text{C}(\text{Tol})\}$  (**14**) being more stable than  $\text{Ti}(\text{N}_2^{\text{ArF}}\text{N}^{\text{Me}})\{\text{N}\{\text{B}(\text{NAr}'\text{CH})_2\}\text{C}(\text{H})\text{C}(\text{Ar}^{\text{F}})\}$  (**16**) relative to the starting **10** and  $\text{ArCCH}$ . Compounds **14** and **16** are susceptible to intramolecular nucleophilic C–F bond cleavage and Ti–F bond formation. Thermolysis of the kinetic products  $\text{Ti}(\text{N}_2^{\text{iPr}}\text{N}^{\text{Me}})\{\text{NHB}(\text{NAr}'\text{CH})_2\}(\text{CCAr}^{\text{F}})$  (**19**) and  $\text{Ti}(\text{N}_2^{\text{NPy}})\{\text{NHB}(\text{NAr}'\text{CH})_2\}(\text{CCAr}^{\text{F}})$  (**23**) converted them to the thermodynamically favored azametallacycles via a 1,2-elimination / [2+2] cycloaddition process, with kinetic and equilibrium isotopes in the expected ranges. DFT calculations on the small model system  $\text{Ti}(\text{N}_2^{\text{SiH}_3}\text{N}^{\text{Py}})\{\text{NB}(\text{NMeCH})_2\}(\text{py})$  (**1Q**) allowed confirmation further interpretation of the kinetic and thermodynamic trends revealed by the experimental data. Finally, although DFT calculations showed that hydroborylation of alkynes (based on  $\text{TolCCH}$  as an example) is thermodynamically feasible, and that the necessary metallacyclic intermediates can be formed, it was not possible for these sterically demanding systems to achieve either a stoichiometric or catalytic synthesis of a borylenamine using the systems described this paper.

Overall, we have reported the first reactions of any Group 4 borylimide, the only previous reactions of this functional group being for a transient scandium borylimide. Current work in our laboratory is aimed at developing this chemistry further with a wider range of substrates, alternative borylimido ligands, and other early transition metals.

## Acknowledgement and Dedication

This work was funded by the EPSRC (grant reference EP/L505031/1) and the University of Oxford SCG Innovation Fund. We thank the University of Oxford's Advanced Research Computing facility for access to supercomputer and other resources. The authors declare no competing financial interests. This paper is dedicated in admiration and friendship to Professor Ernesto Carmona on the occasion of his 70<sup>th</sup> birthday.

## Experimental

Representative syntheses and characterizing data are given below. General experimental procedures, details of starting materials, and syntheses and characterization of all the other new compounds are given in the Supporting Information.

**$\text{Ti}(\text{N}_2^{\text{SiMe}_3}\text{N}^{\text{Me}})\{\text{NB}(\text{NAr}'\text{CH})_2\}(\text{py})$  (**9**).** To a Schlenk flask containing  $\text{Ti}\{\text{NB}(\text{NAr}'\text{CH})_2\}\text{Cl}_2(\text{py})_3$  (**3**, 1.48 g, 1.95 mmol) and  $\text{Li}_2\text{N}_2^{\text{SiMe}_3}\text{N}^{\text{Me}}$  (0.534 g, 1.95 mmol), was added toluene (30 mL) at  $-78^\circ\text{C}$ . The mixture was allowed to warm to room temperature and then stirred for 1 h, after which it had become a dark brown suspension. The volatiles were removed under reduced pressure, and the product extracted into pentane ( $4 \times 20$  mL). Removal of the solvent under reduced pressure, followed by drying *in vacuo*, resulted in **9** as an orange powder. Yield: 1.24 g (79%). Diffraction-

quality crystals were grown from a concentrated hexane solution at 5 °C.  $^1\text{H}$  NMR ( $\text{C}_6\text{D}_6$ , 400.1 MHz):  $\delta$  8.11 (2 H, m, 2,6-py), 7.24 (6 H, overlapping 2  $\times$  m, *m*- and *p*- $\text{C}_6\text{H}_3^i\text{Pr}_2$ ), 6.76 (1 H, m, 4-py), 6.48 (2 H, m, 3,5-py), 5.89 (2 H, s, NCH), 3.77 (4 H, sept.,  $^3J = 6.8$  Hz,  $\text{CHMeMe}$ ), 3.33 (4 H, t,  $^3J = 5.8$  Hz,  $\text{CH}_2\text{NSiMe}_3$ ), 2.61 (2 H, m,  $\text{CH}_2\text{NMe}$ ), 2.29 (2 H, m,  $\text{CH}_2\text{NMe}$ ), 1.66 (3 H, s, NMe), 1.56 (12 H, d,  $^3J = 6.8$  Hz,  $\text{CHMeMe}$ ), 1.32 (12 H, d,  $^3J = 6.8$  Hz,  $\text{CHMeMe}$ ), -0.07 (18 H, s,  $\text{SiMe}_3$ ) ppm.  $^{13}\text{C}\{^1\text{H}\}$  NMR ( $\text{C}_6\text{D}_6$ , 100.6 MHz):  $\delta$  154.0 (2,6-py), 147.9 (*o*- $\text{C}_6\text{H}_3^i\text{Pr}_2$ ), 143.2 (*i*- $\text{C}_6\text{H}_3^i\text{Pr}_2$ ), 137.9 (4-py), 126.7 (*m*- $\text{C}_6\text{H}_3^i\text{Pr}_2$ ), 123.6 (*p*- $\text{C}_6\text{H}_3^i\text{Pr}_2$ ), 123.5 (3,5-py), 117.1 (NCH), 61.2 ( $\text{CH}_2\text{NMe}$ ), 47.9 ( $\text{CH}_2\text{NSiMe}_3$ ), 46.0 (NMe), 28.7 ( $\text{CHMeMe}$ ), 26.1 ( $\text{CHMeMe}$ ), 24.6 ( $\text{CHMeMe}$ ), 1.7 ( $\text{SiMe}_3$ ) ppm.  $^{11}\text{B}\{^1\text{H}\}$  NMR ( $\text{C}_6\text{D}_6$ , 128.4 MHz):  $\delta$  14.9 ppm. IR (NaCl plates, Nujol mull,  $\text{cm}^{-1}$ ): 1930 (w), 1860 (w), 1650 (w), 1602 (s), 1559 (m), 1406 (m), 1340 (w), 1270 (m), 1238 (s), 1213 (w), 1175 (m), 1137 (w), 1089 (m), 1066 (m), 1040 (m), 966 (m), 934 (m), 922 (w), 876 (w), 828 (s), 758 (w), 740 (w), 694 (m), 668 (m), 646 (m). EI-MS:  $m/z = 708$  [ $M - \text{py}$ ] $^+$  (25%). Anal. found (calcd. for  $\text{C}_{42}\text{H}_{70}\text{BN}_7\text{Si}_2\text{Ti}$ ): C, 63.95 (64.02); H, 8.84 (8.96); N, 12.33 (12.44)%.

**$\text{Ti}(\text{N}_2^{\text{SiMe}_3\text{NMe}})\{\text{N}\{\text{B}(\text{NAr}'\text{CH})_2\}\text{C}(\text{H})\text{C}(\text{Tol})\}$  (12).** To a solution of  $\text{Ti}(\text{N}_2^{\text{SiMe}_3\text{NMe}})\{\text{NB}(\text{NAr}'\text{CH})_2\}(\text{py})$  (**9**, 0.291 g, 0.369 mmol) in toluene (10 mL) was added TolCCH (47  $\mu\text{L}$ , 0.369 mmol) at RT, giving an immediate color change to deep red-brown. The reaction mixture was stirred at RT for 1 h, after which the volatiles were removed under reduced pressure, giving **12** as a deep brown, waxy solid. Yield: 0.206 g (68%). Diffraction-quality crystals were grown from a sample of the isolated waxy solid left at RT.  $^1\text{H}$  NMR ( $\text{C}_6\text{D}_6$ , 400.1 MHz):  $\delta$  10.51 (1 H, s,  $\text{TiC}=\text{CH}$ ), 7.23 (2 H, d,  $^3J = 8.0$  Hz, *m*- $\text{C}_6\text{H}_4\text{Me}$ ), 7.18 – 7.11 (6 H, overlapping 2  $\times$  m residual protio solvent resonance, *m*- and *p*- $\text{C}_6\text{H}_3^i\text{Pr}_2$ ), 7.08 (2 H, d,  $^3J = 8.0$  Hz, *o*- $\text{C}_6\text{H}_4\text{Me}$ ), 6.18 (2 H, s, NCH), 3.45 (6 H, overlapping sept. and m,  $\text{CHMeMe}$  and  $\text{CH}_2\text{NSiMe}_3$ ), 3.09 (2 H, m,  $\text{CH}_2\text{NSiMe}_3$ ), 2.65 (2 H, m,  $\text{CH}_2\text{NMe}$ ), 2.15 (3 H, s,  $\text{C}_6\text{H}_4\text{Me}$ ), 2.13 (3 H, s, NMe), 1.92 (2 H, m,  $\text{CH}_2\text{NMe}$ ), 1.30 (12 H, d,  $^3J = 6.9$  Hz,  $\text{CHMeMe}$ ), 1.21 (12 H, d,  $^3J = 6.9$  Hz,  $\text{CHMeMe}$ ), 0.12 (18 H, s,  $\text{SiMe}_3$ ) ppm.  $^{13}\text{C}\{^1\text{H}\}$  NMR ( $\text{C}_6\text{D}_6$ , 100.6 MHz):  $\delta$  205.3 ( $\text{TiC}=\text{CH}$ ), 162.7 ( $\text{TiC}=\text{CH}$ ), 146.5 (*o*- $\text{C}_6\text{H}_3^i\text{Pr}_2$ ), 144.3 (*i*- $\text{C}_6\text{H}_4\text{Me}$ ), 139.7 (*i*- $\text{C}_6\text{H}_3^i\text{Pr}_2$ ), 133.6 (*p*- $\text{C}_6\text{H}_4\text{Me}$ ), 128.7 (*o*- $\text{C}_6\text{H}_4\text{Me}$ ), 128.0 (*p*- $\text{C}_6\text{H}_3^i\text{Pr}_2$ ), 127.6 (*m*- $\text{C}_6\text{H}_4\text{Me}$ ), 124.2 (*m*- $\text{C}_6\text{H}_3^i\text{Pr}_2$ ), 118.9 (NCH), 57.5 ( $\text{CH}_2\text{NMe}$ ), 51.2 ( $\text{CH}_2\text{NSiMe}_3$ ), 43.1 (NMe), 29.0 ( $\text{CHMeMe}$ ), 26.4 ( $\text{CHMeMe}$ ), 23.7 ( $\text{CHMeMe}$ ), 21.2 ( $\text{C}_6\text{H}_4\text{Me}$ ), 2.8 ( $\text{SiMe}_3$ ) ppm.  $^{11}\text{B}\{^1\text{H}\}$  NMR ( $\text{C}_6\text{D}_6$ , 128.4 MHz):  $\delta$  23.8 ppm. IR (NaCl plates, Nujol mull,  $\text{cm}^{-1}$ ): 3406 (w), 1657 (s), 1585 (w), 1504 (m), 1487 (s), 1406 (m), 1362 (s), 1328 (m), 1277 (w), 1245 (s), 1179 (w), 1155 (w), 1117 (s), 1060 (w), 1042 (w), 986 (w), 926 (m), 837 (s), 805 (m), 762 (m), 681 (m), 647 (m). EI-MS:  $m/z = 519$  [ $\text{TolC}(\text{H})\text{C}(\text{H})\text{N}(\text{H})\text{B}(\text{NAr}'\text{CH})_2$ ] $^+$  (92%). Anal. found (calcd. for  $\text{C}_{46}\text{H}_{73}\text{BN}_6\text{Si}_2\text{Ti}$ ): C, 66.82 (66.97); H, 8.84 (8.92); N, 10.01 (10.19)%.

**Ti{MeN(CH<sub>2</sub>CH<sub>2</sub>NAr<sup>F</sup>){CH<sub>2</sub>CH<sub>2</sub>NC<sub>6</sub>F<sub>4</sub>C(Ar<sup>F</sup>)CHNB(NAr'<sup>F</sup>CH)<sub>2</sub>}}(F) (15).** To a solution of Ti(N<sub>2</sub><sup>Ar<sup>F</sup></sup>N<sup>Me</sup>){NB(NAr'<sup>F</sup>CH)<sub>2</sub>}(py) (**10**, 0.300 g, 0.307 mmol) in toluene (10 mL) was added Ar<sup>F</sup>CCH (41 μL, 0.307 mmol) at RT, giving an immediate color change to deep red. The reaction mixture was heated to 60 °C and stirred for 16 h, after which the volatiles were removed under reduced pressure, resulting in a deep brown, waxy solid. Washing with hexane (5 mL) gave **15** as a yellow-orange solid. Yield: 0.191 g (57%). Diffraction-quality crystals were grown from a concentrated C<sub>6</sub>D<sub>6</sub> solution at RT. <sup>1</sup>H NMR (C<sub>6</sub>D<sub>6</sub>, 400.1 MHz): δ 7.29 (2 H, t, <sup>3</sup>J = 7.6 Hz, *p*-C<sub>6</sub>H<sub>3</sub><sup>i</sup>Pr<sub>2</sub>), 7.18 (2 H, d, <sup>3</sup>J = 7.6 Hz, *m<sub>a</sub>*-C<sub>6</sub>H<sub>3</sub><sup>i</sup>Pr<sub>2</sub>), 6.99 (2 H, d, <sup>3</sup>J = 7.6 Hz, *m<sub>b</sub>*-C<sub>6</sub>H<sub>3</sub><sup>i</sup>Pr<sub>2</sub>), 6.72 (1 H, s, NC(H)CAr<sup>F</sup>), 5.89 (2 H, s, NCH), 4.11 (1 H, m, MeNCH<sub>2</sub>CH<sub>2</sub>NC<sub>6</sub>F<sub>4</sub>), 3.31 (4 H, overlapping 2 × sept., CH<sub>a</sub>MeMe and CH<sub>b</sub>MeMe), 3.05 (1 H, m, MeNCH<sub>2</sub>CH<sub>2</sub>NC<sub>6</sub>F<sub>4</sub>), 2.98 (3 H, overlapping 3 × m, MeNCH<sub>2</sub>CH<sub>2</sub>NC<sub>6</sub>F<sub>4</sub>, MeNCH<sub>2</sub>CH<sub>2</sub>NC<sub>6</sub>F<sub>5</sub> and MeNCH<sub>2</sub>CH<sub>2</sub>NC<sub>6</sub>F<sub>5</sub>), 2.72 (1 H, m, MeNCH<sub>2</sub>CH<sub>2</sub>NC<sub>6</sub>F<sub>5</sub>), 2.33 (3 H, s, NMe), 1.99 (1 H, m, MeNCH<sub>2</sub>CH<sub>2</sub>NC<sub>6</sub>F<sub>5</sub>), 1.74 (1 H, m, MeNCH<sub>2</sub>CH<sub>2</sub>NC<sub>6</sub>F<sub>4</sub>), 1.44 (6 H, d, <sup>3</sup>J = 6.8 Hz, CHMe<sub>a</sub>Me), 1.22 (6 H, d, <sup>3</sup>J = 6.8 Hz, CHMe<sub>b</sub>Me), 1.17 (6 H, d, <sup>3</sup>J = 6.8 Hz, CHMeMe<sub>a</sub>), 1.05 (6 H, d, <sup>3</sup>J = 6.8 Hz, CHMeMe<sub>b</sub>) ppm. <sup>13</sup>C{<sup>1</sup>H} NMR (C<sub>6</sub>D<sub>6</sub>, 125.7 MHz): δ 146.8 (*o<sub>a</sub>*-C<sub>6</sub>H<sub>3</sub><sup>i</sup>Pr<sub>2</sub>), 145.8 (*o<sub>b</sub>*-C<sub>6</sub>H<sub>3</sub><sup>i</sup>Pr<sub>2</sub>), 139.1 (*i*-C<sub>6</sub>H<sub>3</sub><sup>i</sup>Pr<sub>2</sub>), 138.4 (NC(H)CAr<sup>F</sup>), 128.4 (*p*-C<sub>6</sub>H<sub>3</sub><sup>i</sup>Pr<sub>2</sub>), 124.1 (*m<sub>a</sub>*-C<sub>6</sub>H<sub>3</sub><sup>i</sup>Pr<sub>2</sub>), 122.9 (*m<sub>b</sub>*-C<sub>6</sub>H<sub>3</sub><sup>i</sup>Pr<sub>2</sub>), 119.8 (NCH), 109.7 (NC(H)CAr<sup>F</sup>), 56.1 (MeNCH<sub>2</sub>CH<sub>2</sub>NC<sub>6</sub>F<sub>5</sub>), 55.7 (MeNCH<sub>2</sub>CH<sub>2</sub>NC<sub>6</sub>F<sub>5</sub>), 53.9 (MeNCH<sub>2</sub>CH<sub>2</sub>NC<sub>6</sub>F<sub>4</sub>), 52.0 (MeNCH<sub>2</sub>CH<sub>2</sub>NC<sub>6</sub>F<sub>4</sub>), 43.5 (NMe), 28.6 (CHMeMe), 26.7 (CHMeMe<sub>b</sub>), 26.5 (CHMeMe<sub>a</sub>), 23.5 (CHMe<sub>a</sub>Me), 22.3 (CHMe<sub>b</sub>Me) ppm. Those resonances belonging to the NAr<sup>F</sup> and C<sub>6</sub>F<sub>4</sub> rings could not be satisfactorily assigned. <sup>11</sup>B{<sup>1</sup>H} NMR (C<sub>6</sub>D<sub>6</sub>, 128.4 MHz): δ 22.4 ppm. <sup>19</sup>F{<sup>1</sup>H} NMR (C<sub>6</sub>D<sub>6</sub>, 376.5 MHz): −100.0 (s, TiF), −134.0 (1 F, dd, <sup>3</sup>J = 24.0 Hz, <sup>4</sup>J = 5.7 Hz, δ-C<sub>6</sub>F<sub>4</sub>), −140.5 (1 F, m, ligand *o*-C<sub>6</sub>F<sub>5</sub>), −142.6 (1 F, br. m, alkene *o*-C<sub>6</sub>F<sub>5</sub>), −142.8 (1 F, d, <sup>3</sup>J = 22.0 Hz, ligand *o*-C<sub>6</sub>F<sub>5</sub>), −145.0 (1 F, dd, <sup>3</sup>J = 20.5 Hz, <sup>4</sup>J = 7.8 Hz, β-C<sub>6</sub>F<sub>4</sub>), −147.0 (1 F, br. m, alkene *o*-C<sub>6</sub>F<sub>5</sub>), −156.0 (1 F, t, <sup>3</sup>J = 21.3 Hz, ligand *p*-C<sub>6</sub>F<sub>5</sub>), −157.5 (1 F, app. t, app. J = 21.4 Hz, α-C<sub>6</sub>F<sub>4</sub>), −160.1 (1 F, br. m, alkene *m*-C<sub>6</sub>F<sub>5</sub>), −162.0 (1 F, t, <sup>3</sup>J = 21.3 Hz, alkene *p*-C<sub>6</sub>F<sub>5</sub>), −162.4 (1 F, app. t, J = 23.5 Hz, γ-C<sub>6</sub>F<sub>4</sub>), −163.0 (2 F, overlapping 2 × m, ligand *m*-C<sub>6</sub>F<sub>5</sub>), −168.5 (1 F, br. m, alkene *m*-C<sub>6</sub>F<sub>5</sub>) ppm. IR (NaCl plates, Nujol mull, cm<sup>−1</sup>): 1637 (w), 1610 (w), 1574 (w), 1521 (s), 1500 (s), 1389 (s), 1345 (m), 1332 (m), 1287 (m), 1208 (w), 1115 (w), 1086 (m), 1023 (m), 996 (s), 986 (s), 944 (w), 910 (w), 901 (w), 886 (w), 857 (w), 811 (w), 758 (m), 738 (m), 691 (m), 656 (m), 600 (m). EI-MS: *m/z* = 1088 [*M*]<sup>+</sup> (1%). Anal. found (calcd. for C<sub>51</sub>H<sub>48</sub>BF<sub>15</sub>N<sub>6</sub>Ti): C, 56.05 (56.27); H, 4.47 (4.44); N, 7.65 (7.72)%.

**Ti(N<sub>2</sub><sup>iPr</sup>N<sup>Me</sup>){NHB(NAr'<sup>F</sup>CH)<sub>2</sub>}(CCAr<sup>F</sup>) (19).** To a solution of Ti(N<sub>2</sub><sup>iPr</sup>N<sup>Me</sup>){NB(NAr'<sup>F</sup>CH)<sub>2</sub>}(py) (**11**, 0.300 g, 0.412 mmol) in hexane (15 mL) was added Ar<sup>F</sup>CCH (55 μL, 0.412 mmol) at RT. The mixture was stirred for 1 h, then the volatiles removed under reduced pressure to yield **19** as a yellow-orange solid. Yield: 0.178 g (51%). <sup>1</sup>H NMR (C<sub>6</sub>D<sub>6</sub>, 400.1 MHz): δ 7.21 – 7.19 (6 H,

overlapping  $2 \times m$  with minor isomer, *m*- and *p*-C<sub>6</sub>H<sub>3</sub><sup>i</sup>Pr<sub>2</sub>), 6.58 (1 H, s, NHB(NAr'CH)<sub>2</sub>), 5.89 (2 H, s, BNCH), 5.00 (2 H, sept., <sup>3</sup>*J* = 6.3 Hz, NCHMeMe), 3.49 (4 H, sept., <sup>3</sup>*J* = 6.9 Hz, C<sub>6</sub>H<sub>3</sub>(CHMeMe)<sub>2</sub>), 3.27 (2 H, m, CH<sub>2</sub>N<sup>i</sup>Pr), 2.87 (2 H, m, CH<sub>2</sub>N<sup>i</sup>Pr), 2.74 (2 H, m, CH<sub>2</sub>NMe), 2.07 (2 H, m, CH<sub>2</sub>NMe), 1.99 (3 H, s, NMe), 1.45 (12 H, d, <sup>3</sup>*J* = 6.9 Hz, C<sub>6</sub>H<sub>3</sub>(CHMeMe)<sub>2</sub>), 1.28 (12 H, d, <sup>3</sup>*J* = 6.9 Hz, C<sub>6</sub>H<sub>3</sub>(CHMeMe)<sub>2</sub>), 1.25 (6 H, d, <sup>3</sup>*J* = 6.3 Hz, NCHMeMe), 0.42 (6 H, d, <sup>3</sup>*J* = 6.3 Hz, NCHMeMe) ppm. <sup>13</sup>C{<sup>1</sup>H} NMR (C<sub>6</sub>D<sub>6</sub>, 125.7 MHz): δ 162.0 (TiCCAr<sup>F</sup>), 148.9 (m, *o*-C<sub>6</sub>F<sub>5</sub>), 147.2 (*o*-C<sub>6</sub>H<sub>3</sub><sup>i</sup>Pr<sub>2</sub>), 140.2 (*i*-C<sub>6</sub>H<sub>3</sub><sup>i</sup>Pr<sub>2</sub>), 138.7 (m, *p*-C<sub>6</sub>F<sub>5</sub>), 136.9 (m, *m*-C<sub>6</sub>F<sub>5</sub>), 124.0 (*m*-C<sub>6</sub>H<sub>3</sub><sup>i</sup>Pr<sub>2</sub>), 123.9 (*p*-C<sub>6</sub>H<sub>3</sub><sup>i</sup>Pr<sub>2</sub>), 117.8 (BNCH), 103.2 (td, <sup>2</sup>*J*<sub>C-F</sub> = 18.9 Hz, <sup>3</sup>*J*<sub>C-F</sub> = 3.7 Hz, *i*-C<sub>6</sub>F<sub>5</sub>), 83.7 (TiCCAr<sup>F</sup>), 57.9 (CH<sub>2</sub>NMe), 52.3 (NCHMeMe), 47.2 (CH<sub>2</sub>N<sup>i</sup>Pr), 45.8 (NMe), 28.8 (C<sub>6</sub>H<sub>3</sub>(CHMeMe)<sub>2</sub>), 24.9 (C<sub>6</sub>H<sub>3</sub>(CHMeMe)<sub>2</sub>), 24.1 (C<sub>6</sub>H<sub>3</sub>(CHMeMe)<sub>2</sub>), 21.1 (NCHMeMe), 19.6 (NCHMeMe) ppm. <sup>11</sup>B{<sup>1</sup>H} NMR (C<sub>6</sub>D<sub>6</sub>, 128.4 MHz): 23.0 ppm. <sup>19</sup>F{<sup>1</sup>H} NMR (C<sub>6</sub>D<sub>6</sub>, 376.5 MHz): -138.9 (2 F, m, *o*-C<sub>6</sub>F<sub>5</sub>), -159.1 (1 F, t, <sup>3</sup>*J* = 21.7 Hz, *p*-C<sub>6</sub>F<sub>5</sub>), -164.4 (2 F, m, *m*-C<sub>6</sub>F<sub>5</sub>). IR (NaCl plates, Nujol mull, cm<sup>-1</sup>): 3484 (w), 3409 (m), 3208 (w), 2094 (w, ν(C≡C)), 1596 (m), 1512 (s), 1493 (s), 1416 (s), 1398 (s), 1339 (s), 1277 (m), 1181 (m), 1140 (m), 1109 (m), 1060 (m), 991 (s), 959 (s), 938 (m), 905 (w), 868 (w), 824 (m), 787 (m), 758 (s), 713 (w), 658 (m), 630 (w), 605 (m). EI-MS: *m/z* = 595 [Ar<sup>F</sup>C(H)C(H)N(H)B(NAr'CH)<sub>2</sub>]<sup>+</sup> (<1%). Anal. found (calcd. for C<sub>45</sub>H<sub>62</sub>BF<sub>5</sub>N<sub>6</sub>Ti): C, 64.02 (64.29); H, 7.56 (7.43); N, 9.91 (10.00)%.

**Supporting Information Available:** Details of starting materials. Remaining details of the synthesis and characterizing data for new compounds, and kinetic experiments, as detailed above. Further details of the crystal structure determinations, including X-ray data collection and processing parameters and further data in CIF format. This information is available free of charge *via* the internet at <http://pubs.acs.org>. The supporting information file contains the computed Cartesian coordinates of all of the molecules reported in this study. The file may be opened as a text file to read the coordinates, or opened directly by a molecular modelling program such as Mercury (version 3.3 or later, <http://www.ccdc.cam.ac.uk/pages/Home.aspx>) for visualization and analysis. The CCDC codes for the structures in this paper are: CCDC 1575707–1575717.

## References

1. For reviews see: (a) Wigley, D. E. *Prog. Inorg. Chem.* **1994**, 42, 239-482; (b) Duncan, A. P.; Bergman, R. G. *Chem. Rec.* **2002**, 2, 431-445; (c) Mountford, P. *Chem. Commun.* **1997**, 2127-2134; (d) Gade, L. H.; Mountford, P. *Coord. Chem. Rev.* **2001**, 216-217, 65-97; (e) Hazari, N.; Mountford, P. *Acc. Chem. Res.* **2005**, 38, 839-849; (f) Bolton, P. D.; Mountford, P. *Adv. Synth. Catal.* **2005**, 347, 355-366; (g) Fout, A. R.; Kilgore, U. J.; Mindiola, D. J. *Chem. - Eur. J.* **2007**, 13, 9428-9440; (h) Odom, A. L. *Dalton Trans.* **2005**, 225-233; (i)



- Schafer, L. L.; Lee, A. V. *Eur. J. Inorg. Chem.* **2007**, 2243-2255; (j) Müller, T. E.; Hultsch, K. C.; Yus, M.; Foubelo, F.; Tada, M. *Chem. Rev.* **2008**, *108*, 3795-3892; (k) Lorber, C. *Coord. Chem. Rev.* **2016**, *308*, 76-96; (l) Wolczanski, P. T. *Organometallics* **2018**, *37*, 505-516.
2. For a highlight and review see: (a) Mindiola, D. J. *Angew. Chem., Int. Ed.* **2008**, *47*, 1557-1559; (b) Dilworth, J. R. *Coord. Chem. Rev.* **2017**, *330*, 53-94.
  3. (a) Kool, L. B.; Rausch, M. D.; Alt, H. G.; Herberhold, M.; Hill, A. F.; Thewalt, U.; Wolf, B. *J. Chem. Soc., Chem. Commun.* **1986**, 408-409; (b) Polse, J. L.; Kaplan, A. W.; Andersen, R. A.; Bergman, R. G. *J. Am. Chem. Soc.* **1998**, *120*, 6316-6328; (c) Kaplan, A. W.; Polse, J. L.; Ball, G. E.; Andersen, R. A.; Bergman, R. G. *J. Am. Chem. Soc.* **1998**, *120*, 11649-11662; (d) Hanna, T. E.; Keresztes, I.; Lobkovsky, E.; Bernskoetter, W. H.; Chirik, P. J. *Organometallics* **2004**, *23*, 3448-3458; (e) Tiong, P. J.; Groom, L. R.; Clot, E.; Mountford, P. *Chem. - Eur. J.* **2013**, *19*, 4198-4216.
  4. (a) Walsh, P. J.; Hollander, F. J.; Bergman, R. G. *J. Am. Chem. Soc.* **1988**, *110*, 8729-8731; (b) Cummins, C. C.; Baxter, S. M.; Wolczanski, P. T. *J. Am. Chem. Soc.* **1988**, *110*, 8731-8733.
  5. (a) Danopoulos, A. A.; Redshaw, C.; Vaniche, A.; Wilkinson, G.; Hussain-Bates, B.; Hursthouse, M. B. *Polyhedron* **1993**, *12*, 1061-1071; (b) Weber, K.; Korn, K.; Schorm, A.; Kipke, J.; Lemke, M.; Khvorost, A.; Harms, K.; Sundermeyer, J. *Z. Anorg. Allg. Chem.* **2003**, *629*, 744-754.
  6. Fryzuk, M. D.; MacKay, B. A.; Johnson, S. A.; Patrick, B. O. *Angew. Chem., Int. Ed.* **2002**, *14*, 3709-3712.
  7. Thompson, R.; Chen, C.-H.; Pink, M.; Wu, G.; Mindiola, D. J. *J. Am. Chem. Soc.* **2014**, *136*, 8197-8200.
  8. (a) Stevenson, L. C.; Mellino, S.; Clot, E.; Mountford, P. *J. Am. Chem. Soc.* **2015**, *137*, 10140-10143; (b) Mellino, S.; Stevenson, L. C.; Clot, E.; Mountford, P. *Organometallics* **2017**, *36*, 3329-3342.
  9. Grant, L. N.; Pinter, B.; Kurogi, T.; Carroll, M. E.; Wu, G.; Manor, B. C.; Carroll, P. J.; Mindiola, D. J. *Chem. Sci.* **2017**, *8*, 1209-1224.
  10. Clough, B. A.; Mellino, S.; Protchenko, A. V.; Slusarczyk, M.; Stevenson, L. C.; Blake, M. P.; Xie, B.; Clot, E.; Mountford, P. *Inorg. Chem.* **2017**, *56*, 10794-10814.
  11. Hadlington, T. J.; Abdalla, J. A. B.; Tirfoin, R.; Aldridge, S.; Jones, C. *Chem. Commun.* **2016**, *52*, 1717-1720.

12. Clough, B. A.; Mellino, S.; Clot, E.; Mountford, P. *J. Am. Chem. Soc.* **2017**, *139*, 11165-11183.
13. (a) Bettinger, H. F. *J. Am. Chem. Soc.* **2006**, *128*, 2534-2535; (b) Bettinger, H. F.; Bornemann, H. *J. Am. Chem. Soc.* **2006**, *128*, 11128-11134.
14. Pieper, W.; Schmitz, D.; Paetzold, P. *Chem. Ber.* **1981**, *114*, 3801-3812.
15. (a) Bettinger, H. F. *Inorg. Chem.* **2007**, *46*, 5188-5195; (b) Bettinger, H. F.; Filthaus, M.; Bornemann, H.; Oppel, I. M. *Angew. Chem., Int. Ed.* **2008**, *47*, 4744-4747; (c) Bettinger, H. F.; Filthaus, M.; Neuhaus, P. *Chem. Commun.* **2009**, 2186-2188; (d) Filthaus, M.; Schwertmann, L.; Neuhaus, P.; Seidel, R. W.; Oppel, I. M.; Bettinger, H. F. *Organometallics* **2012**, *31*, 3894-3903; (e) Müller, M.; Maichle-Mössmer, C.; Bettinger, H. F. *Chem. Commun.* **2013**, *49*, 11773-11775.
16. (a) Polse, J. L.; Andersen, R. A.; Bergman, R. G. *J. Am. Chem. Soc.* **1998**, *120*, 13405-13414; (b) Ward, B. D.; Maisse-Francois, A.; Mountford, P.; Gade, L. H. *Chem. Commun.* **2004**, 704-705; (c) Vujkovic, N.; Ward, B. D.; Maisse-Francois, A.; Wadepohl, H.; Mountford, P.; Gade, L. H. *Organometallics* **2007**, *26*, 5522-5534; (d) Schofield, A. D.; Nova, A.; Selby, J. D.; Manley, C. D.; Schwarz, A. D.; Clot, E.; Mountford, P. *J. Am. Chem. Soc.* **2010**, *132*, 10484-10497; (e) Schwarz, A. D.; Onn, C. S.; Mountford, P. *Angew. Chem., Int. Ed.* **2012**, *51*, 12298-12302.
17. (a) Bytschkov, I.; Doye, S. *Eur. J. Org. Chem.* **2003**, 935-946; (b) Pohlki, F.; Doye, S. *Chem. Soc. Rev.* **2003**, *32*, 104-114; (c) Doye, S. *Synlett* **2004**, 1653-1672; (d) Hultsch, K. C. *Adv. Synth. Catal.* **2005**, *347*, 367-391; (e) Zeng, X. *Chem. Rev.* **2013**, *113*, 6864-6900; (f) Walsh, P. J.; Baranger, A. M.; Bergman, R. G. *J. Am. Chem. Soc.* **1992**, *114*, 1708-1719.
18. (a) Vujkovic, N.; Fillol, J. L.; Ward, B. D.; Wadepohl, H.; Mountford, P.; Gade, L. H. *Organometallics* **2008**, *27*, 2518-2528; (b) Blake, A. J.; Collier, P. E.; Gade, L. H.; Mountford, P.; Lloyd, J.; Pugh, S. M.; Schubart, M.; Skinner, M. E. G.; Trösch, J. M. *Inorg. Chem.* **2001**, *40*, 870-877; (c) Pugh, S. M.; Trösch, D. J. M.; Wilson, D. J.; Bashall, A.; Cloke, F. G. N.; Gade, L. H.; Hitchcock, P. B.; McPartlin, M.; Nixon, J. F.; Mountford, P. *Inorg. Chem.* **2000**, *19*, 3205; (d) Bashall, A.; Collier, P. E.; Gade, L. H.; McPartlin, M.; Mountford, P.; Pugh, S. M.; Radojevic, S.; Schubart, M.; Scowen, I. J.; Trösch, D. J. M. *Organometallics* **2000**, *19*, 4784-4894; (e) Schofield, A. D.; Nova, A.; Selby, J. D.; Schwarz, A. D.; Clot, E.; Mountford, P. *Chem. - Eur. J.* **2011**, *17*, 265-285; (f) Tiong, P. J.; Schofield, A. D.; Selby, J. D.; Nova, A.; Clot, E.; Mountford, P. *Chem. Commun.* **2010**, *46*, 85-87; (g) Selby, J. D.; Manley, C. D.; Schwarz, A. D.; Clot, E.; Mountford, P. *Organometallics* **2008**, *27*, 6479-6494; (h) Selby, J. D.; Manley, C. D.; Feliz, M.; Schwarz, A. D.; Clot, E.;

- Mountford, P. *Chem. Commun.* **2007**, 4937-4939; (i) Gehrman, T.; Scholl, S. A.; Fillol, J. L.; Wadepohl, H.; Gade, L. H. *Chem. - Eur. J.* **2012**, *18*, 3925-3942; (j) Gehrman, T.; Fillol, J. L.; Scholl, S. A.; Wadepohl, H.; Gade, L. H. *Angew. Chem., Int. Ed.* **2011**, *50*, 5757-5761; (k) Gehrman, T.; Fillol, J. L.; Wadepohl, H.; Gade, L. H. *Angew. Chem., Int. Ed.* **2009**, *48*, 2152-2156; (l) Herrmann, H.; Fillol, J. L.; Wadepohl, H.; Gade, L. H. *Angew. Chem., Int. Ed.* **2007**, *46*, 8426-8430.
19. Ward, B. D.; Orde, G.; Clot, E.; Cowley, A. R.; Gade, L. H.; Mountford, P. *Organometallics* **2004**, *23*, 4444-4461.
  20. Fletcher, D. A.; McMeeking, R. F.; Parkin, D. J. *Chem. Inf. Comput. Sci.* **1996**, *36*, 746-759 (The UK Chemical Database Service: CSD version updated Feb 2018).
  21. Addison, A. W.; Rao, T. N.; Reedijk, J.; van Rijn, J.; Verschoor, G. C. *J. Chem. Soc., Dalton Trans.* **1984**, 1349-1356.
  22. Nguyen, T. T.; Kortman, G. D.; Hull, K. L. *Organometallics* **2016**, *35*, 1713-1725.
  23. Lorenzo, S.; Lewis, G. R.; Dance, I. *New J. Chem.* **2000**, *24*, 295-304.
  24. (a) Kiplinger, J. L.; Richmond, T. G.; Osterberg, C. E. *Chem. Rev.* **1994**, *94*, 373-431; (b) Scholl, S. A.; Plundrich, G. T.; Wadepohl, H.; Gade, L. H. *Inorg. Chem.* **2013**, *52*, 10158-10166; (c) Groom, L. R.; Russell, A. F.; Schwarz, A. D.; Mountford, P. *Organometallics* **2014**, *33*, 1002-1009.
  25. Hunter, C. A.; Lawson, K. R.; Perkins, J.; Urch, C. J. *J. Chem. Soc., Perkin Trans. 2* **2001**, 651-669.
  26. Patrick, C. R.; Prosser, G. S. *Nature* **1960**, *187*, 1021.
  27. Lozman, O. R.; Bushby, R. J.; Vinter, J. G. *J. Chem. Soc., Perkin Trans. 2* **2001**, 1446-1452.
  28. Polse, J. L.; Andersen, R. A.; Bergman, R. G. *J. Am. Chem. Soc.* **1995**, *117*, 5393-5394.
  29. Blake, R. E.; Antonelli, D. M.; Henling, L. M.; Schaefer, W. P.; Hardcastle, K. I.; Bercaw, J. E. *Organometallics* **1998**, *17*, 718.
  30. Hoyt, H. M.; Bergman, R. G. *Angew. Chem., Int. Ed.* **2007**, *46*, 5580-5582.
  31. Hartwig, J. F.; Cook, K. S.; Hapke, M.; Incarvito, C. D.; Fan, Y.; Webster, C. E.; Hall, M. B. *J. Am. Chem. Soc.* **2005**, *127*, 2538-2552.
  32. (a) Bennett, J. L.; Wolczanski, P. T. *J. Am. Chem. Soc.* **1997**, *119*, 10696-10719; (b) Cummins, C. C.; Schaller, C. P.; Van Duyne, G. D.; Wolczanski, P. T.; Chan, A. W. E.; Hoffmann, R. *J. Am. Chem. Soc.* **1991**, *113*, 2985-2994; (c) Schaller, C. P.; Cummins, C. C.; Wolczanski, P. T. *J. Am. Chem. Soc.* **1996**, *118*, 591-611; (d) Slaughter, L. M.; Wolczanski, P. T.; Klinckman, T. R.; Cundari, T. R. *J. Am. Chem. Soc.* **2000**, *122*, 7953-7975; (e) Hanna, T. E.; Lobkovsky, E.; Chirik, P. J. *Inorg. Chem.* **2007**, *46*, 2359-2361.

33. (a) Gómez-Gallego, M.; Sierra, M. A. *Chem. Rev.* **2011**, *111*, 4857-4963; (b) Balcells, D.; Clot, E.; Eisenstein, O. *Chem. Rev.* **2010**, *110*, 749-823.
34. (a) Lowry, T. H.; Richardson, K. S., *Mechanism and Theory in Organic Chemistry*. Harper and Row: New York, 1987; (b) Carpenter, B. K., *Determination of Reaction Mechanisms*. Wiley-Interscience: New York, 1984.
35. Parkin, G. *Acc. Chem. Res.* **2009**, *42*, 315-325.
36. (a) Clot, E.; Mégret, C.; Eisenstein, O.; Perutz, R. N. *J. Am. Chem. Soc.* **2006**, *128*, 8350-8357; (b) Bigmore, H. R.; Meyer, J.; Krummenacher, I.; Rüegger, H.; Clot, E.; Mountford, P.; Breher, F. *Chem. - Eur. J.* **2008**, *14*, 5918-5934.
37. (a) Schock, L. E.; Marks, T. J. *J. Am. Chem. Soc.* **1988**, *110*, 7701-7715; (b) Bryndza, H. E.; Fong, K. F.; Paciello, R. A.; Tam, W.; Bercaw, J. E. *J. Am. Chem. Soc.* **1987**, *109*, 1444-1456; (c) Holland, P. L.; Andersen, R. A.; Bergman, R. G.; Huang, J.; Nolan, S. P. *J. Am. Chem. Soc.* **1997**, *119*, 12800-12814; (d) Holland, P. L.; Andersen, R. A.; Bergman, R. G. *Comments. Inorg. Chem.* **1999**, *21*, 115-129.
38. Weitershaus, K.; Ward, B. D.; Kubiak, R.; Muller, C.; Wadepohl, H.; Doye, S.; Gade, L. H. *Dalton Trans.* **2009**, 4586-4602.
39. (a) Straub, B. F.; Bergman, R. G. *Angew. Chem., Int. Ed.* **2001**, *40*, 4632-4635; (b) Tillack, A.; Jiao, H.; Garcia Castro, I.; Hartung, C. G.; Beller, M. *Chem. - Eur. J.* **2004**, *10*, 2409-2420; (c) Tobisch, S. *Dalton Trans.* **2006**, 4277-4285; (d) Tobisch, S. *Chem. - Eur. J.* **2007**, *13*, 4884 – 4894; (e) Müller, C.; Koch, R.; Doye, S. *Chem. - Eur. J.* **2008**, *14*, 10430-10436; (f) Tobisch, S. *Chem. - Eur. J.* **2008**, *14*, 8590 – 8602.